Interference phenomena in coherent active spectroscopy of light scattering and absorption: holographic multidimensional spectroscopy

N. I. Koroteev

M. V. Lomonosov State University, Moscow

Usp. Fiz. Nauk **152**, 493–520 (July 1987)

Studies are reviewed on the development and applications of a new method of recording optical spectra that preserves full information on both the amplitude and phase relationships between the spectral components of the light field being recorded, and which thus realizes "holographic spectroscopy." The method has been realized in practice in various polarization modifications of Coherent Active (anti-Stokes) Raman Spectroscopy (CARS). By using it, the problem has been solved in principle of resolving close, overlapping spectral lines not amenable to discrimination by the Rayleigh criterion in noncoherent spectra. In polarization CARS the experimenter can carry out a controlled action on the form and amplitude of an optical resonance being recorded ("multidimensionality" of spectra). However, this is not accompanied by an actual distortion of the spectrum or action from the probe field on the object of study. The principles of holographic spectroscopy have been realized experimentally, and by using them new information has been obtained on the internal structure of broad superposed Raman and light-absorption lines.

TABLE OF CONTENTS

1. INTRODUCTION

The traditional forms of optical spectroscopy, based on measuring luminescence, absorption, and light-scattering spectra, have played a very appreciable role in modern science and technology, owing to their unique diagnostic potentialities and high information content. At the same time they possess a cardinal defect that arises from the very method of using them to extract the information on the object of study. This consists in measuring the spectral distribution of the *intensity* of the light absorbed, reradiated, and/ or scattered by the object. We can say that, as in optics before the invention of holography, the "phase problem" remains unsolved in traditional optical spectroscopy—the problem of reconstructing complete information on the object being studied from data incomplete in principle that are contained in the spectral distribution of the intensity of the light field after interacting with the object.

As has been elucidated in recent years, the lacking phase information, which is completely lost in recording ordinary optical spectra, can be extracted from the data of coherent active spectroscopy of light scattering and/or absorption. A method can be realized in the latter of complete recording of both the amplitude and phase relationships between the spectral components of the coherently scattered light field (or, as is the same, recording the real and imaginary parts of the field simultaneously). That is, a method has been realized that can be called holographic spectroscopy.

Just as in ordinary holography, here the complete recording of the spectral information is performed by interference of the coherent spectral components of the light field being studied with the specially introduced radiation of a coherent background (or one initially present in the radiation leaving the object being studied), which plays the role of the reference wave. In other words, in coherent active spectroscopy one can realize a scheme of heterodyning the signal, while the amplitude and phase of the reference ("heterodyning") light wave can be optimized for maximally complete recording and subsequent readout of the amplitude and phase information contained in the signal wave.

Among the undoubted achievements of this relatively

 0038-5670/87/070628-16$01.80

new and as yet rarely employed method of coherent spectroscopy are the solution in principle by using it of the problem of discriminating close, overlapping spectral lines corresponding to physically differing optical resonances that cannot be resolved according to the Rayleigh criterion.[1,2] In favorable situations in coherent active spectroscopy, one can resolve even optical resonances having identical frequencies and shapes of spectral lines (but differing, e.g., in width and/or polarization characteristics).[3]

Of course, in achieving complete recording of the actual physical information on a medium being studied in all schemes of active spectroscopy, the coherence of the signal light wave leaving the medium has fundamental significance. This is enabled by the coherence of the light waves emitted by the phased elementary molecular oscillators of this medium. In turn, the phasing of the molecular (atomic, ionic, etc.) oscillators is enabled by the stimulated nature of the vibrations of the nuclei and/or the optical electrons in the shells of these elementary emitters. Here the amplitude and phase of the cited vibrations are fixed by the amplitudes and phases of the coherent light waves (pump and probe) that are specially introduced into the medium while performing experiments in coherent active spectroscopy.

The principle of coherent active spectroscopy can be explained with the example of Raman spectra by using Fig. 1. The overall scheme of obtaining the signal in active spectroscopy is very similar to that of dynamic holography[1)]: Two light beams with plane phase fronts (wave vectors $\mathbf{k}_1$ and $\mathbf{k}_2$) intersect in a nonlinear medium and "write" a plane hologram. That is, they produce a plane diffraction grating

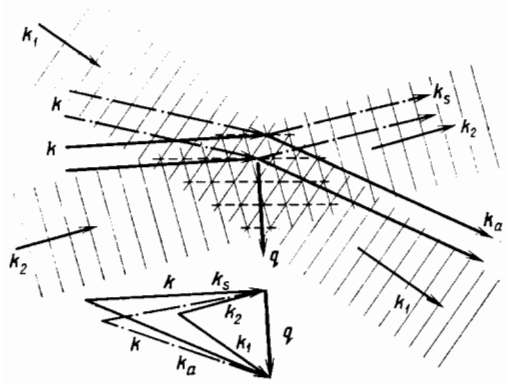

FIG. 1. Principle of coherent active Raman spectroscopy from the standpoint of optical induction of a running diffraction grating. Reflection of the probe wave $\mathbf{k}$ occurs at an angle determined by the Bragg condition (the diagram below explains the relationships between the wave vectors). Owing to the Doppler effect, the reflected waves have a frequency shifted with respect to the frequency ω of the probe ray by $\pm\Delta\omega = \pm(\omega_1 - \omega_2)$. The diffraction gratings involving the coherent wave of intramolecular vibrations and the wave of coherent perturbations of the electron shells of the molecules have identical frequencies ($\Delta\omega = \omega_1 - \omega_2$) and wave vectors ($\mathbf{q} = \mathbf{k}_1 - \mathbf{k}_2$). Therefore the Stokes (ω_s, $\mathbf{k}_s$) and anti-Stokes (ω_a, $\mathbf{k}_a$) components of the diffraction field contain both an information-bearing component (involving diffraction by the former of the mentioned gratings) and a reference component (or "heterodyne" component, involving diffraction by gratings of the latter type). Just as in ordinary holography, the interference of the information-bearing and the reference components of the coherently scattered waves during recording of the spectra enables one to reconstruct complete information about the properties and structure of the coherent wave of intramolecular vibrations, i.e., solve the "phase problem" of vibrational molecular spectroscopy. In the lower diagram: $\mathbf{k}_s$ is the dot-dash line, and $\mathbf{k}_a$ the solid line.

(wave vector $\mathbf{q} = \mathbf{k}_1 - \mathbf{k}_2$), that diffracts a probe light beam (wave vector $\mathbf{k}$). Diffraction is most efficient when synchronization conditions are satisfied between the wave vectors of the diffracted components of the probe beam $\mathbf{k}_s$ and $\mathbf{k}_a$ and the wave vectors of the waves "writing" and "reading out" the dynamic hologram:

$$\mathbf{k}_s = \mathbf{k} - \mathbf{q} \equiv \mathbf{k} - (\mathbf{k}_1 - \mathbf{k}_2), \tag{1a}$$

$$\mathbf{k}_a = \mathbf{k} + \mathbf{q} = \mathbf{k} + (\mathbf{k}_1 - \mathbf{k}_2). \tag{1b}$$

Evidently these conditions are equivalent to the Bragg diffraction conditions in holography.

However, an essential difference between the diffraction scheme in active spectroscopy and the ordinary holographic scheme is the fact that the waves having $\mathbf{k}_1$ and $\mathbf{k}_2$ that "write" the hologram (in active spectroscopy they are called the pump waves) have different frequencies $\omega_1 \neq \omega_2$, so that the grating $\mathbf{q}$ oscillates with the frequency $\Delta\omega = \omega_1 - \omega_2$ and travels in the medium with the phase velocity $\mathbf{v}_{ph} = \mathbf{q}(\omega_1 - \omega_2)|\mathbf{k}_1 - \mathbf{k}_2|^{-2} = \mathbf{q}\Delta\omega|\mathbf{q}|^{-2}$. Correspondingly, the diffraction of the probe beam by this running grating leads to a Doppler shift of the frequency of the diffracted components (they are respectively called the Stokes and anti-Stokes components):

$$\omega_s = \omega - \mathbf{q}\mathbf{v}_\Phi = \omega - \Delta\omega = \omega - (\omega_1 - \omega_2), \tag{2a}$$

$$\omega_a = \omega + \mathbf{q}\mathbf{v}_\Phi = \omega + \Delta\omega = \omega + (\omega_1 - \omega_2). \tag{2b}$$

In active spectroscopy one measures the intensity (and also the polarization and phase) of the Stokes and/or the anti-Stokes components as functions of $\Delta\omega = \omega_1 - \omega_2$ while the Bragg conditions (1a) and (1b) are fulfilled. Whenever $\Delta\omega$ coincides with any eigenfrequency Ω_σ of the intramolecular vibrations (or other internal micromovements of the medium being studied) that are active in Raman scattering: $\Delta\omega \approx \Omega_\sigma$, the efficiency of diffraction of the probe wave undergoes a resonance variation.

The latter can be interpreted as the resonance excitation in the medium of a pair of harmonic pump waves of the running wave of coherent intramolecular vibrations and subsequent scattering by this wave [with shift of frequency into the Stokes or anti-Stokes region in line with (2a) and (2b)] of the plane monochromatic probe light wave while the synchronization conditions (1a) and (1b) are fulfilled. Here the existence of a nonzero intensity of diffraction of the probe wave in the nonresonance case (although generally smaller than under resonance conditions), i.e., with a detuning $\Delta\omega$ far from all the resonance frequencies Ω_σ of the medium, is associated with the excitation in the electron shells of the molecules of the medium of stimulated (hence coherent) nonresonance oscillations of the optical electrons. The emission of the latter undergoes interference and yields a nonresonance component of the diffraction of the probe beam. Evidently, when the resonance condition $\Delta\omega = \Omega_\sigma$ is satisfied, both diffraction components are present in the coherently scattered radiation and can interfere with one another. The nonresonance diffraction component amounts to the coherent background in the active spectrum against which the resonance lines lie that correspond to the intramolecular vibrations and other optically active resonances of the medium.

In coherent spectroscopy the experimenter can exert a

controlled action of the shape and amplitude of the optical resonance being recorded, as is used for more complete, high-contrast recording.[2-4] This is attained by controlled variation of the conditions of recording the spectra, i.e., the conditions of interference of the coherent background and the information-bearing components of the spectrum under study. Most often one uses for these purposes a variation of the polarization condition,[2-4] since the polarization characteristics of the coherent background and the information-bearing diffraction components generally differ. Here it is important to stress that appreciable variations of the shape of the spectral line of the studied resonance in this case are not associated with an actual distorting action from the probe light field on the object of study, in contrast, e.g., to absorption-saturation spectroscopy.[5]

Just as in holography the recorded image is a volume image and can be examined at different angles,[7] so in polarization active spectroscopy the optical resonances being studied can be recorded in different manifestations, so that the contour of the spectral line can be varied in controlled fashion over a very broad range.[6,8-15]

Figure 2 shows a family of panoramic spectra of coherent Raman scattering in a liquid obtained by using holographic Raman spectroscopy. The measured quantity in all the spectra is the intensity $I_{a\|}(\Delta\omega)$ coherently scattered under conditions of Bragg diffraction (1) of the light wave with the anti-Stokes frequency $\omega_a = 2\omega_1 - \omega_2$ after passing through a polarizing analyzer, as a function of the pump frequency difference $\Delta\omega = \omega_1 - \omega_2$. The position of the transmission plane of the analyzer (it is given by the unit vector $\mathbf{e}_a$ in the diagram above the figure) differs for the spectra of Fig. 2a–e, and is altered by rotating the analyzer about an axis passing along the anti-Stokes ray; the angle ε characterizes the deviation of $\mathbf{e}_a$ from the direction orthogonal to the linear polarization of the coherent background. (As is shown in the diagram, the polarization unit vectors $\mathbf{e}_1$ and $\mathbf{e}_2$ of the pump waves having the frequencies ω_1 and ω_2 are respectively separated from one another by the angle $\varphi = 60°$.) The change in ε alters the interference conditions of the coherent background and the information-bearing diffraction components, as is expressed in a cardinal change in the shape of the spectral line of each of at least three optical resonances of the medium being studied that lie in the range of study—in this case the normal vibrations of different conformers of molecules of *n*-pentane having the frequencies $\Omega_\sigma/2\pi c \sim 872$, ~ 868, and ~ 845 cm^{-1}. A joint study of all the spectra of the type of Fig. 2a–e enables one for the first time to conduct a complete measurement of the vibrational spectrum of this liquid, and in particular, to associate the doublet 872–868 cm^{-1} with the trans–trans and trans–gauche rotational isomers of *n*-pentane (in the spontaneous Raman spectra the group of lines at 872–868 cm^{-1} looks like a continuous unresolved band); see Refs. 11 and 30 and Fig. 9 in Sec. 4 of this article.

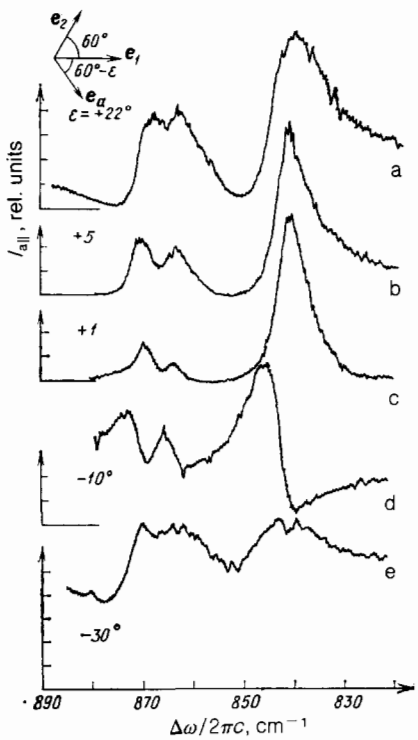

FIG. 2. Polarization CARS spectra of liquid *n*-pentane at $T = 240$ K (see also Fig. 9). Spectra *a*-*e* differ in the value of the angle ε (shown next to the curves) between the normal to the polarization direction of the nonresonance background $\mathbf{P}^{NR}$ and the plane of transmission of the polarizing analyzer in the anti-Stokes ray. The polarization diagram of the interaction is shown on the top.

One can interpret the spectra of Fig. 2a–e as individual two-dimensional cross sections of a multidimensional manifold that represents the optical resonances being studied in an abstact "spectrooptical space." These same results can be treated as a change of "vantage point" of the experimenter over the set of optical resonances being studied. This manifests the effect of holographic extensive content of information in coherent active spectroscopy.

As will be shown below, the spectra of Fig. 2a–e, which differ so much among themselves, just like the analogous sets of polarization active Raman spectra of other transparent, isotropic liquids and gases, can be represented as derivatives of a limited number of independent invariants—functions of the frequency-detuning $\Delta\omega$, which are the real and imaginary parts of three independent components of the fourth-order tensor of the nonlinear optical third-order susceptibility $\chi^{(3)}_{ijkl}(\omega_a; \omega, \omega_1, -\omega_2) = \chi^{(3)}_{ijkl}(\Delta\omega)$.[2)] The reconstruction of the spectral course of these functions from an arbitrarily large number of different experimental spectra like Fig. 2a–e is the method of extracting the maximally complete information (within the framework of the problem formulated) on the Raman-active medium being studied. The second stage in solving the inverse spectral problem in this formulation becomes the extraction from the given parameters obtained in the first stage of the individual resonances (central frequencies, form factors of lines, polarization and symmetry characteristics, etc.) forming the studied spectral bands by mutual superposition.

Of course, one can formulate the inverse spectral problem, and in many cases solve it successfully, without adducing complete spectral information on the optical resonances being studied. In particular, in spontaneous Raman spectroscopy for *isolated lines*, one can completely determine all the parameters of the corresponding optical resonances (including data on the trace and invariants of the symmetric and antisymmetric components of the Raman polarizability tensor) on the basis of the traditional methods alone, which are based on the noncoherent interaction of light with mat-

ter. However, upon approach and overlap in the spectrum of individual lines, the problem of spectral resolution of broad bands within the framework of traditional noncoherent spectroscopy becomes ever more ambiguous, while the formulation of the inverse spectral problem becomes false.[32–38,54,55] Precisely in these cases the adduction of extra spectroscopic information contained in the results of complete measurements by the methods of coherent active spectroscopy becomes important in principle.[2–4,6,8–15]

In speaking of solving the phase problem in spectroscopy, we have dealt mainly, and shall do so below, with vibrational spectroscopy, and more exactly—with Raman spectroscopy in homogeneous, isotropic media. However, also other forms of spectroscopy, in particular absorption spectroscopy in the infrared, ultraviolet, and visible ranges, can be supplemented by coherent analogs that enable performing complete measurements. In studying absorption spectra in the infrared and visible ranges, the methods of coherent active spectroscopy of light absorption[6,40,45] prove highly information-rich. Just like active Raman spectroscopy, they are based on measuring the frequency dispersion of the cubic optical susceptibility $\chi^{(3)}_{ijkl}(\omega_a; \omega, \omega_1, -\omega_2)$. However, in contrast to active Raman spectroscopy, it is not the difference of pump frequencies that tunes into resonance with the transition being studied, but one of them (ordinarily ω_2), which is scanned over the studied absorption band. Here also the polarization modifications of the coherent methods prove most effective. An example of applying them to the problem of resolving the internal structure of an electronic absorption band of a solution of a neodymium salt is found in Sec. 5 of this review.

The aim of this article is a condensed, but rather thorough presentation of the principles of holographic multidimensional spectroscopy and their demonstration with examples of the experimental resolution of the internal stucture of broad overlapping spectral bands of Raman scattering and single-photon absorption in pure liquids and solutions.

We should stress that, although the idea itself of complete measurements in coherent active spectroscopy had already been formulated seveal years ago[1–4] (in its most complete form, in the book of Ref. 6), only in the last few years have several series of experiments[8–15] been performed, which have demonstrated with exceptional perspicuity the unique potentialities of holographic spectroscopy.

2. INTERFERENCE NATURE OF COHERENT LIGHT-SCATTERING SPECTRA. RELATIONSHIP WITH SPONTANEOUS RAMAN SPECTROSCOPY

The key problem of holographic spectroscopy is to obtain a coherent response from the medium being studied; as has already been stated in the Introduction, it can be solved in the scheme of coherent active spectroscopy of light scattering and absorption.[6]

At first, for the sake of definiteness, we shall restrict the treatment to coherent active spectroscopy of Raman scattering in isotropic, homogeneous, nonabsorbing media (transparent gases and liquids). There the information on the contour of the resonance curve of the molecular vibrations is extracted from the spectral dependence of the amplitude, phase, and polarization characteristics of the anti-Stokes (ω_a) and Stokes (ω_s) components [see (2a) and (2b)] as obtained by scanning $\Delta\omega$ near Ω: $\omega_a = \omega + (\omega_1 - \omega_2)$, $\omega_s = \omega - (\omega_1 - \omega_2)$.

In the presentation below, the following situation, as we have already mentioned in the Introduciton, will be very important. Simultaneously with the excitation of a running grating of intramolecular vibrations in the medium, always a pure phase running grating of the refractive index is also formed. It involves the nonlinearity of the electronic subsystem of the molecules and has the same frequency $\Delta\omega$ and the same wave vector $\mathbf{q}$ as the former grating. In the nonresonance case all the characteristics of the second lattice remain invariant upon scanning $\Delta\omega$. The diffraction by it of the probe wave yields the coherent background that plays the role of the reference wave in holographic spectroscopy or the heterodyne wave in the scheme of optical heterodyning, since the Stokes and anti-Stokes diffraction components [again their parameters are given by (1a), (1b), (2a), and (2b)] are completely coherent with respect to the corresponding light waves diffracted by the wave of intramolecular vibrations. The interference of the coherent background and the information-bearing diffraction components makes possible complete recording of the spectral information on the optical mode of the material being studied—in this case, on the real and imaginary parts (or in other words, on the synphase and quadrature components) of the coherent response of the molecules of the medium to the biharmonic excitation.

It is worth noting that initially the presence of a coherent background in coherent Raman spectra was evaluated as an especially negative feature of coherent spectroscopy, which leads to the appearance of a relatively high pedestal for the Raman lines being studied, and which hinders the study of weak lines and overtones.[16–18] Only after our studies[2–4] presenting the methods of controlled suppression of the coherent background and the active shaping of the contour of Raman spectral lines was the qualitative specifics of the interference nature of the shape of coherent Raman spectral lines reevaluated in its favor.

In nonlinear spectroscopy the coherent optical response of the medium being studied—the nonlinear polarizability—is characterized phenomenologically by using the nonlinear third-order optical susceptibilities. For the most widespread variant of active spectroscopy with recording of the anti-Stokes component, which is called coherent anti-Stokes Raman spectroscopy (CARS), the complex amplitude of the wave of the anti-Stokes cubic polarization $\mathbf{P}(\omega_a)$ is expressed in terms of the complex amplitudes of the vectors of the electric-field intensities of the light waves $\mathbf{E}(\omega)$, $\mathbf{E}_1(\omega_1)$, and $\mathbf{E}_2(\omega_2)$ at the frequencies ω, ω_1, and ω_2, correspondingly as follows[1,6,17]:

$$P_j(\omega_a) = D\chi^{(3)}_{ijkl}(\omega_a; \omega, \omega_1, -\omega_2) E_j E_{1k} E_2^*. \qquad (3)$$

Here and everywhere below, we assume summation over the repeated tensor indices from 1 to 3; the numerical coefficient D takes account of possible frequency degeneracy ($D = 6$ if $\omega \neq \omega_1$, and $D = 3$ if $\omega = \omega_1$), while $\chi^{(3)}_{ijkl}(\omega_a; \omega, \omega_1, -\omega_2)$ is the spectral component of the third-order nonlinear optical susceptibility tensor.

When the adiabatic (Born-Oppenheimer) approximation is applicable, the latter quantity has two components, one of which involves the resonance coherent response of the vibrational subsystem of the molecule (termed $\chi^{(3)R}_{ijkl}$ below),

while the other involves the nonresonance coherent response of the electronic subsystem, $\chi^{(3)NR}_{ijkl}$:

$$\chi^{(3)}_{ijkl}(\omega_a;\ \omega,\ \omega_1,\ -\omega_2) = \chi^{(3)R}_{ijkl} + \chi^{(3)NR}_{ijkl}. \quad (4)$$

One can perform a microscopical calculation of the quantities $\chi^{(3)R}_{ijkl}$ and $\chi^{(3)NR}_{ijkl}$ within the framework of quantum perturbation theory in the third order in the Hamiltonian of the dipole interaction of the field with the medium (for more details see Refs. 6, 20, and 21). The existence of the two components in (4) is equivalent to the above-mentioned excitation in the studied medium of two types of running diffraction gratings. The nonlinear polarizability of (3) acts as the source of the field in the Maxwell equations. Under the synchronization conditions of (1a) it gives rise to a plane monochromatic light wave at the anti-Stokes frequency[6,16,17]:

$$E_i(\omega_a) \sim P_i(\omega_a). \quad (5)$$

The intensity of the anti-Stokes wave measured experimentally has the form

$$I_a \sim E_i(\omega_a) E_i^*(\omega_a)$$

$$\sim |\chi^{(3)}_{ijkl}(\omega_a;\ \omega,\ \omega_1,\ \omega_2)\, e^*_{ai} e_j e_{1k} e^*_{2l}|^2 I_1 I_2. \quad (6)$$

Here we have introduced the unit polarization vectors and intensities of the pump waves having the frequencies ω_1 and ω_2 ($\mathbf{e}_1$, $\mathbf{e}_2$ and I_1, I_2), of the probe wave having the frequency $\omega(\mathbf{e}, I)$, and of the anti-Stokes wave being recorded ($\mathbf{e}_a$, I_a), respectively.

The expression (6) with allowance for (4) is the fundamental relationship employed in holographic spectroscopy. Let us put it into a more compact form by using the properties of macroscopic symmetry of the media that we are interested in—isotropic, nonchiral, homogeneous liquids and gases belonging to the limiting class $\infty\infty m$.[6,22,23] In them, only 21 of the 81 components of the tensor $\chi^{(3)}_{ijkl}$ differ from zero, and only 3 are independent:

$$\chi^{(3)}_{iijj} = \chi^{(3)}_{1122},\quad \chi^{(3)}_{ijij} = \chi^{(3)}_{1212},\quad \chi^{(3)}_{ijji} = \chi^{(3)}_{1221},\quad \chi^{(3)}_{iiii} = \chi^{(3)}_{1111}$$

$$(i,\ j = 1,\ 2,\ 3,\ \text{but } i \neq j), \quad (7)$$

Here the isotropy condition is fulfilled:

$$\chi^{(3)}_{1122} + \chi^{(3)}_{1212} + \chi^{(3)}_{1221} = \chi^{(3)}_{1111}. \quad (8)$$

Upon introducing the scalar product of the complex unit vectors $\mathbf{e}_\alpha$ and $\mathbf{e}_\beta$ according to the rule

$$(\mathbf{e}_\alpha,\ \mathbf{e}_\beta) = e_{\alpha i} e_{\beta i},$$

we can assign the following invariant form to Eq. (6) by using (7) and (8):

$$I_a(\omega_a) \sim |\chi^{(3)}_{1122}(\mathbf{e}^*_a\mathbf{e})(\mathbf{e}_1\mathbf{e}^*_2) + \chi^{(3)}_{1212}(\mathbf{e}^*_a\mathbf{e}_1)(\mathbf{e}\mathbf{e}^*_2) + \chi^{(3)}_{1221}(\mathbf{e}^*_a\mathbf{e}^*_2)(\mathbf{e}\mathbf{e}_1)|^2 I_1 I_2. \quad (9)$$

The sequence of frequency arguments of the susceptibilities entering into (8) and (9) is always the same: $\omega_a; \omega, \omega_1, -\omega_2$.

Although the cubic nonlinear susceptibility tensor individually satisfies the isotropy condition (8) for both components—the resonance Raman component $\chi^{(3)R}_{ijkl}$ and the nonresonance electronic component $\chi^{(3)NR}_{ijkl}$—the relationships between the nonzero, linearly independent components $\chi^{(3)R}_{ijkl}$ and $\chi^{(3)NR}_{ijkl}$ generally differ. In a transparency band for the frequencies ω and $\omega_{1,2,a}$ and far from two-photon resonances at the frequencies $\omega + \omega_1$, $\omega_a + \omega_2$, and $\omega - \omega_2$, the components of $\chi^{(3)NR}_{ijkl}$ are real and they satisfy the so-called Kleinman relationships[1,6,21,24]:

$$\chi^{(3)NR}_{1111} = 3\chi^{(3)NR}_{1212} = 3\chi^{(3)NR}_{1122} = 3\chi^{(3)NR}_{1221}. \quad (10)$$

The relationships between the components of $\chi^{(3)R}_{ijkl}$ (which are generally complex) are determined by the symmetry properties of the normal vibrations that are excited.

Under the same conditions in which (10) is satisfied, the components of $\chi^{(3)R}_{ijkl}(\omega_a; \omega, \omega_1, -\omega_2)$ prove to be functions of a single frequency argument—the frequency difference $\Delta\omega = \omega_1 - \omega_2 = \omega_a - \omega$. Further, the nonlinear fluctuation-dissipation theorem (FDT) holds, according to which the cross section for Stokes spontaneous Raman scattering in different polarization configurations proves to be proportional to the imaginary components of the corresponding components of $\chi^{(3)R}_{ijkl}$[6,25,60]:

$$\left(\frac{d^2\sigma}{do\, d(\Delta\omega)}\right)_\parallel \sim \frac{\operatorname{Im}\chi^{(3)R}_{1111}(\Delta\omega)}{\exp(-\hbar\Delta\omega/kT)-1}, \quad (11a)$$

$$\left(\frac{d^2\sigma}{do\, d(\Delta\omega)}\right)_\perp \sim \frac{\operatorname{Im}(\chi^{(3)R}_{1212}(\Delta\omega)}{\exp(-\hbar\Delta\omega/kT)-1}, \quad (11b)$$

$$\left(\frac{d^2\sigma}{do\, d(\Delta\omega)}\right)_\otimes \sim \frac{\operatorname{Im}(\chi^{(3)R}_{1212}(\Delta\omega)+\chi^{(3)R}_{1221}(\Delta\omega))}{\exp(-\hbar\Delta\omega/kT)-1}. \quad (11c)$$

Here $d^2\sigma/dod(\Delta\omega)$ is the differential Raman cross-section in the "forward" geometry per unit solid angle and unit spectral interval, while the symbols $\parallel$, $\perp$, and $\otimes$ attached to the symbols of the cross-sections indicate the polarization configuration: $\parallel$—the unit vectors of the exciting and the spontaneously scattered radiations are linear and parallel to one another; $\perp$—they are linear and orthogonal; $\otimes$—the exciting and scattered radiations are polarized circularly in mutually opposed directions.

Thus in standard spontaneous Raman spectroscopy, which operates with the spectral distribution of the intensity of the light scattered by the fluctuational intramolecular movements, only the imaginary parts of the corresponding spectral components of the response functions of the medium can be measured—the resonance (Raman) cubic susceptibilties $\chi^{(3)R}_{ijkl}$. In active Raman spectroscopy, and in particular, in CARS spectroscopy, owing to the coherence of the scattering process and the existence of the nonzero real background nonlinearities $\chi^{(3)NR}_{ijkl}$ corresponding to the nonresonance response of the electronic subsystem of the molecule, the measured spectral dependences of the intensity of the coherently scattered signal will contain data on the dispersion of both the imaginary and the real parts of $\chi^{(3)R}_{ijkl}$, and also on their relative signs.

One can extact from the experimentally measured dispersion curves $I_a(\Delta\omega)$ the sought *complete* information on the medium, i.e., reconstruct all three complex functions of the frequency mismatch $\chi^{(3)R}_{1122}(\Delta\omega)$, $\chi^{(3)R}_{1212}(\Delta\omega)$, and $\chi^{(3)R}_{1221}(\Delta\omega)$ by varying the conditions of interference in the signal being recorded between the resonance and nonresonance contributions by changing the polarizations of the in-

teracting light waves and the polarization conditions of recording the coherent spectra.

3. CONTROLLED SHAPING OF THE SPECTRAL CONTOUR OF AN OPTICAL RESONANCE IN COHERENT ACTIVE SPECTROSCOPY

One can actively shape the contour of a spectral line in amplitude-polarization (AP) active Raman spectroscopy and in pure polarization active Raman spectroscopy (also called coherent Raman ellipsometry—CRE[1,2,6,26,27]). Here one uses the difference of the polarization characteristics of the coherent background and the information-bearing scattering components, which is expressed in the difference in the relationships between the nonzero components of the susceptibilities $\chi_{ijkl}^{(3)\mathrm{NR}}$ and $\chi_{ijkl}^{(3)\mathrm{R}}$.

In line with what we have said and upon using (9), one can easily understand that one can vary the conditions of recording (i.e., vary the polarization unit vector $\mathbf{e}_a$ of the anti-Stokes wave being recorded, e.g., by putting a polarization analyzer with variable orientation in front of the photodetector), in order to vary the amplitude and phase of the coherent background with respect to the information-bearing components of the spectrum, and thus shape the contour of the resonance spectral line.

To extract complete information on the resonance being studied, i.e., on the dispersion curves of the real and imaginary parts of all three independent components of the tensor $\chi_{ijkl}^{(3)\mathrm{R}}$, one must perform a series of several measurements of the spectra $I_a(\Delta\omega)$ for different mutual orientations of the polarization unit vectors $\mathbf{e}_a$ and $\mathbf{e}$, $\mathbf{e}_1$, $\mathbf{e}_2$.

Figure 3 shows the polarization diagram of the mutual orientations of these unit vectors for the case of arbitrary linear polarizations of all (the collinear) waves having the frequencies ω, $\omega_{1,2,a}$.

The vector of the nonresonance electronic polarization

$$\mathbf{P}^{\mathrm{NR}} = \chi_{1122}^{(3)\mathrm{NR}}\mathbf{e}\,(\mathbf{e}_1\mathbf{e}_2^*) + \chi_{1212}^{(3)\mathrm{NR}}\mathbf{e}_1\,(\mathbf{e}\mathbf{e}_2^*) + \chi_{1221}^{(3)\mathrm{NR}}\mathbf{e}_2^*\,(\mathbf{e}\mathbf{e}_1) \qquad (12)$$

forms the angle Φ with the vector $\mathbf{e}_1$:

$$\Phi = \operatorname{arctg}\frac{\chi_{1122}^{(3)\mathrm{NR}}\cos\varphi\sin\psi + \chi_{1221}^{(3)\mathrm{NR}}\sin\varphi\cos\psi}{\chi_{1111}^{(3)\mathrm{NR}}\cos\varphi\cos\psi + \chi_{1212}^{(3)\mathrm{NR}}\sin\varphi\sin\psi}. \qquad (13)$$

We can introduce into the treatment the isolated Raman resonance characterized by the complex form factor of the spectral line $f(\Delta\omega)$ common to all three independent components of the susceptibility $\chi_{ijkl}^{(3)\mathrm{R}}$:

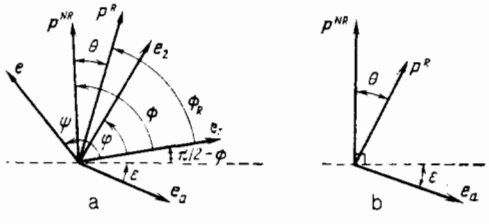

FIG. 3. Mutual orientation of the vectors fixing the linear polarization of the pump waves of CARS ($\mathbf{e}_1$, $\mathbf{e}_2$), the probe wave ($\mathbf{e}$), and the anti-Stokes signal wave ($\mathbf{e}_a$) (all the light waves are assumed to be plane and propagating along a direction perpendicular to the plane of the drawing) (a); the vectors $\mathbf{P}^{\mathrm{NR}}$ and $\mathbf{P}^{\mathrm{R}}$ defined by Eqs. (12) and (17) and the vector $\mathbf{e}_a$. The angle ε is measured from the direction orthogonal to $\mathbf{P}^{\mathrm{NR}}$, and the angle θ from the direction of $\mathbf{P}^{\mathrm{NR}}$.

$$\chi_{ijkl}^{(3)\mathrm{R}}(\Delta\omega) = \bar{\chi}_{ijkl}^{(3)\mathrm{R}} f(\Delta\omega). \qquad (14)$$

Here $\bar{\chi}_{ijkl}^{(3)\mathrm{R}}$ is a real quantity that has the meaning of the peak value (in the center of the line where $\Delta\omega = \Omega$) of the corresponding component of the resonance Raman susceptibility tensor, $|f(\Delta\omega = \Omega)| = 1$.

For a resonance of Lorentzian form we have

$$f(\Delta\omega) = \frac{1}{-i-\Delta}. \qquad (15)$$

Here we have $\Delta = (\omega_1 - \omega_2 - \Omega)/\Gamma$, where Γ is the half-width of the resonance curve at the level 0.5 of the maximum.

We recall that the ratio

$$\rho = \frac{\bar{\chi}_{1212}^{(3)\mathrm{R}}}{\bar{\chi}_{1111}^{(3)\mathrm{R}}} \qquad (16)$$

coincides with the degree of depolarization of an isolated Raman line defined in spontaneous Raman spectroscopy.[1,6]

As we see from Fig. 3, such an isolated resonance can be depicted by the vector

$$\mathbf{P}^{\mathrm{R}} = \bar{\chi}_{1122}^{(3)\mathrm{R}}\mathbf{e}\,(\mathbf{e}_1\mathbf{e}_2^*) + \bar{\chi}_{1212}^{(3)\mathrm{R}}\mathbf{e}_1\,(\mathbf{e}\mathbf{e}_2^*) + \bar{\chi}_{1221}^{(3)\mathrm{R}}\mathbf{e}_2^*\,(\mathbf{e}\mathbf{e}_1), \qquad (17)$$

that forms the angle

$$\Phi_{\mathbf{R}} = \operatorname{arctg}\frac{\rho'\cos\varphi\sin\psi + \bar{\rho}\sin\varphi\cos\psi}{\cos\varphi\cos\psi + \rho\sin\varphi\sin\psi} \qquad (18)$$

with the vector $\mathbf{e}_1$. In this formula we have introduced the parameters

$$\rho' = \frac{\bar{\chi}_{1122}^{(3)\mathrm{R}}}{\bar{\chi}_{1111}^{(3)\mathrm{R}}}, \quad \bar{\rho} = \frac{\bar{\chi}_{1221}^{(3)\mathrm{R}}}{\bar{\chi}_{1111}^{(3)\mathrm{R}}}. \qquad (19)$$

(The parameters, $\bar{\rho}'$ coincides with the degree of depolarization ρ if the corresponding Raman tensor is symmetric.[6])

Thus the resonance Raman component $\mathbf{P}^{\mathrm{R}}$ and the nonresonance electronic component $\mathbf{P}^{\mathrm{NR}}$, which comprise the nonlinear source at the anti-Stokes frequency $\mathbf{P}(\omega_a)$, are generally collinear (see Fig. 3b). The corresponding angle θ between them is

$$\theta = \Phi - \Phi_{\mathbf{R}}. \qquad (20)$$

Evidently the formulas given above, which were derived for the general case of CARS with nondegenerate frequencies ($\omega \neq \omega_1 \neq \omega_2$) remain valid also in the more widespread degenerate scheme of CARS ($\omega = \omega_1$, $\omega_a = 2\omega_1 - \omega_2$), if we set $\mathbf{e} = \mathbf{e}_1$ and $\psi = 0$ in it and allow for the extra symmetry of $\chi_{ijkl}^{(3)\mathrm{R}}(\omega_a; \omega_1, \omega_1, -\omega_2)$ in the two middle indices.

One can attain full suppression of the coherent background by choosing a special orientation of the polarization conditions of recording (i.e., the vector $\mathbf{e}_a$):

$$(\mathbf{e}_a, \mathbf{P}^{\mathrm{NR}}) = 0. \qquad (21)$$

In this case the intensity of the CARS signal will depend only on two (of the three) independent combinations of the components of $\chi_{ijkl}^{(3)\mathrm{R}}$ [28]:

$$I_{a,\mathrm{R}} \sim |(\mathbf{P}^{\mathrm{R}}, \mathbf{e}_a)|^2 \sim |(\chi_{1122}^{(3)\mathrm{R}} - b_1\chi_{1221}^{(3)\mathrm{R}}) + (\chi_{1212}^{(3)\mathrm{R}} - b_2\chi_{1221}^{(3)\mathrm{R}})|^2 II_1I_2, \qquad (22)$$

Here we have

$$b_1 = \frac{\chi_{1122}^{(3)\mathrm{NR}}}{\chi_{1221}^{(3)\mathrm{NR}}}, \quad b_2 = \frac{\chi_{1212}^{(3)\mathrm{NR}}}{\chi_{1221}^{(3)\mathrm{NR}}}.$$

(With fulfillment of the Kleinman conditions of (10) we have $b_1 = b_2 = 1$.)

If the polarization analyzer in the recording channel is turned in a direction away from that given by (21) (i.e., we set $\varepsilon \neq 0$), then the signal transmitted through the analyzer will contain also a nonresonance component. The shape of the dispersion curve results from the interference of the projections of the nonlinear sources $\mathbf{P}^{NR}$ and $\mathbf{P}^{R}$ on the transmission direction of the analyzer:

$$\frac{I_{a\parallel}(\Delta\omega)}{II_1I_2} \sim |\chi^{(3)}(\Delta\omega)|^2$$

$$= ||\mathbf{P}^{NR}|\sin\varepsilon + f(\Delta\omega)|\,\mathbf{P}^{R}|\sin(\varepsilon-\theta)|^2. \qquad (23)$$

Here we have introduced the complex nonlinear coupling coefficient

$$\chi^{(3)}(\Delta\omega) \equiv \chi^{(3)}_{ijkl}(\Delta\omega)\, e_{ai}e_je_{1k}e^*_{2l} = \chi^{(3)\prime} + i\chi^{(3)\prime\prime}. \qquad (24)$$

The character of the interference is determined by the relative phase of the terms entering into (23), which in turn depends on the angles ε and $\varepsilon - \theta$. Thus, a scheme of optical heterodyning is realized in CARS. For a resonance of Lorentzian form we obtain the following from (23):

$$\frac{I_{a\parallel}(\Delta\omega)}{II_1I_2} \sim |\chi^{(3)}(\Delta\omega)|^2 \sim \sin^2\varepsilon - 2$$

$$\times \sin\varepsilon\sin(\varepsilon-\theta)\frac{\alpha\Delta}{1+\Delta^2} + \frac{[\alpha\sin(\varepsilon-\theta)]^2}{1+\Delta^2}. \qquad (25)$$

Here we have introduced the "strength" of the Raman resonance

$$\alpha = \frac{|\mathbf{P}^{R}|}{|\mathbf{P}^{NR}|}. \qquad (26)$$

As we see from (25), by choosing ε either from the interval from 0 to θ or outside it, one can substantially change the shape of the resonance being recorded, since the interference minima in the relationship $I_{a\parallel}(\Delta\omega) \sim |\chi^{(3)}(\Delta\omega)|^2$ in these two cases lie on opposite sides of the maximum. One says that a shift of the trough has occurred (an effect first found in Ref. 2).

The interference effects in amplitude-polarization CARS are commonly analyzed qualitatively by using the geometric concept of the nonlinear coupling coefficient $\chi^{(3)}(\Delta\omega)$ in the complex plane[2,6] (Fig. 4).

The circle 1 in Fig. 4 is the geometric locus of the complex vectors $\chi^{(3)}$ when the polarization analyzer is set in the anti-Stokes ray for the maximum transmission of the "coherent background," i.e., with $\varepsilon = \pi/2$. The vectors $|\chi^{(3)}|_{max}$ and $|\chi^{(3)}|_{min}$ having the maximum and minimum length, corresponding to the maximum and minimum intensity in the CARS spectrum, are shown. Curve 2 is the $\chi^{(3)}(\Delta\omega)$ relationship with complete suppression of the coherent background: $\varepsilon = 0$. The pedestal in the active spectrum is absent. Curve 3 is the $\chi^{(3)}(\Delta\omega)$ relationship when the analyzer is set close to complete suppression of the resonance contribution to the CARS signal: $\varepsilon \approx \theta$ (we assume, as in Fig. 1, that $\theta < 0$). Here the trough in the $I_a(\Delta\omega)$ relationship lies on the other side of the maximum from cases 1 and 4 (evidently for exact equality $\varepsilon = 0$ $I_{a\parallel}(\Delta\omega) = \text{const}$). Finally, curve 4 is the $\chi^{(3)}(\Delta\omega)$ relationship for maximum transmission of the resonance component of the CARS signal: $\varepsilon = \theta - (\pi/2)$.

Also the contours of the dispersion dependences of the

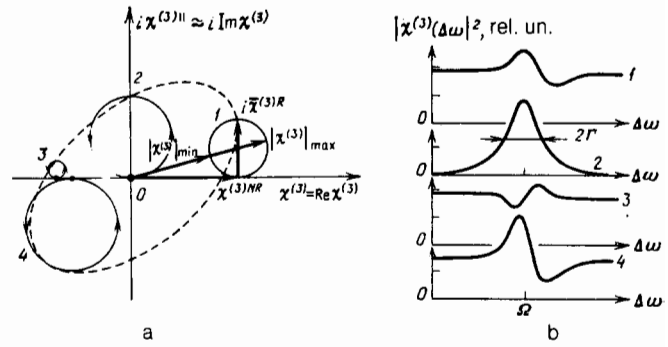

Fig. 4. a—Geometric representation of the nonlinear coupling coefficient of (24) for an isolated resonance of Lorentzian form $\chi^{(3)} = \chi^{(3)\prime} + i\chi^{(3)\prime\prime}$ in the complex plane for different orientations of the polarizing prism used to shape the contour of the optical resonance being recorded (circles marked by the numbers 1–4; for curve 1 the real nonresonance contribution $\chi^{(3)NR}$ and the resonance contribution $i\bar{\chi}^{(3)R}$ (purely imaginary in the center of the line) to the overall nonlinear coupling coefficient $\chi^{(3)}$ are shown separately. Also shown are the complex vectors of $\chi^{(3)}$ having a maximum, $|\chi^{(3)}|_{max}$, and minimum, $|\chi^{(3)}|_{min}$ value of the square of the modulus. As $\Delta\omega \to \infty$, $\chi^{(3)}(\Delta\omega)$ acquires purely real values equal to $\chi^{(3)NR}$ ($i\chi^{(3)\prime\prime} = i\,\mathrm{Im}\chi^{(3)}$; along the axis of abscissas we have $\chi^{(3)\prime} = \mathrm{Re}\,\chi^{(3)}$). b—Frequency dispersion relationships $|\chi^{(3)}(\Delta\omega)|^2 \sim I_a(\Delta\omega)$, corresponding to circles 1–4 in Fig. a.

parameters of the polarization ellipse of the coherent anti-Stokes signal are amenable to controlled shaping as $\Delta\omega$ passes through resonance in the scheme of coherent Raman ellipsometry.[4,6]

The simplest method, and at the same time the closest to that presented above, for active shaping of the contour of a spectral line being measured in coherent Raman ellipsometry (CRE) is based on a method proposed by Oudar *et al.*[27] for measuring the ellipticity parameters of the anti-Stokes signal. In it the ellipticity is measured by spatial separation (using a polarizing prism) of the elliptically polarized beam into two linearly polarized beams having orthogonal polarization directions, and subsequent measurement of their intensity ratio as a function of the frequency detuning $\Delta\omega$: $I_{a\parallel}(\Delta\omega)/I_{a\perp}(\Delta\omega)$. Rotation of the polarizing prism about the axis of the beam (again one can characterize it by the angle ε introduced above) alters $I_{a\parallel}(\Delta\omega)$ and $I_{a\perp}(\Delta\omega)$ and thus affects their ratio.

This method is distinguished by its practicality and convenience, since actually it amounts to a scheme for normalizing the intensity of the anti-Stokes signal transmitted through the polarizing prism to the intensity of the orthogonally polarized component of the same ray reflected by this prism. Thus, an internal standard always exists in the described normalization scheme. This enables one to eliminate practically completely the disturbing influence of amplitude fluctuations of the pump waves and the probe wave on the accuracy of measurements of the spectral contour of the resonance of the medium.

The ratio of intensities of the orthogonally polarized components of the anti-Stokes signal measured in this CRE method is expressed in terms of the parameters of an isolated resonance introduced above and the angle ε:

$$\frac{I_{a\parallel}(\Delta\omega)}{I_{a\perp}(\Delta\omega)} = \left|\frac{\sin\varepsilon + f(\Delta)\,\alpha\sin(\varepsilon-\theta)}{\cos\varepsilon + f(\Delta)\,\alpha\cos(\varepsilon-\theta)}\right|^2. \qquad (27)$$

The dependence of the measured ratio on the frequency in

CRE proves more complex than in amplitude-polarization CARS, since generally both the numerator and the denominator demonstrate resonance behavior. However, also here the contour of the resonance being measured is amenable to active shaping by varying the angle ε.

In the case of an isolated resonance of Lorentzian form in (15), the simplest contour of the dependence being measured is again obtained for $\varepsilon = 0$, i.e., with complete suppression of the coherent background in the anti-Stokes radiation transmitted through the polarizing prism:

$$\frac{I_{a\parallel}(\Delta\omega)}{I_{a\perp}(\Delta\omega)} = \frac{(\alpha \sin\theta)^2}{1+(\Delta-\alpha\cos\theta)^2}. \tag{28}$$

We see that the spectrum of the ratio $I_{a\parallel}/I_{a\perp}$ again has a Lorentzian form with a width 2Γ and with a maximum shifted from the position of exact resonance ($\Delta\omega = \Omega$) by the amount $\alpha\Gamma\cos\theta$ (on the wave number scale). When one rotates the prism by a nonzero angle ε the shape of the spectral line of the signal becomes complicated: it acquires in explicit form an imprint of the interference of the resonance and nonresonance contributions.

4. INTERFERENCE OF OPTICAL RESONANCES IN COHERENT ACTIVE SPECTRA

If a medium under study possesses not one, but N different resonances having central frequencies $\Omega_1, \Omega_2, \ldots$ and form factors of the lines $f_1(\Delta_1), f_2(\Delta_2), \ldots$, then the cubic optical susceptibility tensor of this medium will contain the corresponding number of resonance components:

$$\chi^{(3)}_{ijkl}(\omega_a;\ \omega,\ \omega_1,\ -\omega_2) = \chi^{(3)\mathrm{NR}}_{ijkl} + \sum_{\sigma=1}^{N} f_\sigma(\Delta_\sigma)\,\bar{\chi}^{(3)\mathrm{R}\sigma}_{ijkl}. \tag{29}$$

Here we have $\Delta_\sigma = (\omega_1 - \omega_2 - \Omega_\sigma)/\Gamma_\sigma$, and Γ_σ is the half-width of the resonance at the frequency Ω_σ.

When one introduces a polarizing prism into the anti-Stokes ray, the intensity of the CARS signal passing through it is written as follows, by analogy with (23):

$$\frac{I_{a\parallel}(\Delta\omega)}{II_1I_2} \sim |\chi^{(3)}(\Delta\omega)|^2 = \Big| |\mathbf{P}^{\mathrm{NR}}| \sin\varepsilon + \sum_{\sigma=1}^{N} f_\sigma(\Delta_\sigma)\,|\mathbf{P}^{\mathrm{R}\sigma}| \sin(\varepsilon-\theta_\sigma)\Big|^2. \tag{30}$$

Here $\chi^{(3)}(\Delta\omega)$ is defined in (24), and we have

$$\mathbf{P}^{\mathrm{R}\sigma} = \bar{\chi}^{(3)\mathrm{R}\sigma}_{1122}\mathbf{e}(\mathbf{e}_1\mathbf{e}_2^*) + \bar{\chi}^{(3)\mathrm{R}\sigma}_{1212}\mathbf{e}_1(\mathbf{e}\mathbf{e}_2^*) + \bar{\chi}^{(3)\mathrm{R}\sigma}_{1221}\mathbf{e}_2^*(\mathbf{e}\mathbf{e}_1). \tag{31}$$

As before, ε is the angle between the normal to the vector $\mathbf{P}^{\mathrm{NR}}$ and the plane of the vibrations transmitted by the polarizing prism, while θ_σ is the angle between $\mathbf{P}^{\mathrm{NR}}$ and $\mathbf{P}^{\mathrm{R}\sigma}$. Analogously to (27), in this case we can write the following expression for the shape of the spectral line of the CRE signal:

$$\frac{I_{a\parallel}(\Delta\omega)}{I_{a\perp}(\Delta\omega)} = \left| \frac{\sin\varepsilon + \sum_{\sigma=1}^{N} f_\sigma(\Delta_\sigma)\,\alpha_\sigma \sin(\varepsilon-\theta_\sigma)}{\cos\varepsilon + \sum_{\sigma=1}^{N} f_\sigma(\Delta_\sigma)\,\alpha_\sigma \cos(\varepsilon-\theta_\sigma)} \right|^2. \tag{32}$$

Here we have

$$\alpha_\sigma = \frac{|\mathbf{P}^{\mathrm{R}\sigma}|}{|\mathbf{P}^{\mathrm{NR}}|}.$$

Thus, in line with what we have said in Secs. 2 and 3, the shape of the spectral line in the polarization variants of active Raman spectroscopy results from the interference of the contributions of different resonances among themselves and with the coherent background (and not simply from superposition of the spectral lines, as happens in the traditional noncoherent forms of spectroscopy). Therefore, by choosing the polarization conditions of observation, one can alter the character of the interference of the resonance (i.e., information-bearing) and nonresonance (background) contributions in the recorded signal, while gaining the most complete information on the resonances being studied and, in particular, the most contrast-rich spectral resolution of close-lying lines that merge into a continuous band in the ordinary way of taking spectra.

Let us turn to the very simple case of superposition of two close-lying but physically differing isolated resonances, i.e., resonances having close-lying (or even coincident) central frequencies Ω_1 and Ω_2, but differing in the set of components of the tensors $\chi^{\mathrm{R}\sigma(3)}_{ijkl}$ and/or form factors of the lines $f_\sigma(\Delta_\sigma)$.

We can easily see from what we have said above that the most contrast-rich resolution of the close-lying lines should be expected in polarization active Raman spectroscopy lines when the coherent background has a phase and amplitude such that the relative phases of the interfering resonances are opposite, while their amplitudes are close to one another.

Figure 5 shows a diagram explaining the principle of resolving a doublet of superposed lines in the amplitude-polarization variant of CARS. Curve 1 is the geometric locus of $\chi^{(3)}(\Delta\omega)$ for a pair of close-lying lines of Lorentzian form having the same width 2Γ that are still resolvable by the Rayleigh criterion ($|\Omega_1 - \Omega_2| > 2\Gamma$), but characterized by contributions to $\chi^{(3)}$ differing in phase by π. Curves 2, 2′, and 2″ are the analogous trajectories described by the ends of $\chi^{(3)}(\Delta\omega)$ upon scanning $\Delta\omega$ in the case of close-lying resonances ($|\Omega_1 - \Omega_2| < \Gamma$) for different magnitudes and relative signs of $\chi^{(3)\mathrm{NR}}$. As the lines approach closer ($|\Omega_1 - \Omega_2| \to 0$), the curve 2 is compressed, while keeping its form. Therefore the spectra of $|\chi^{(3)}(\Delta\omega)|^2$ do not change

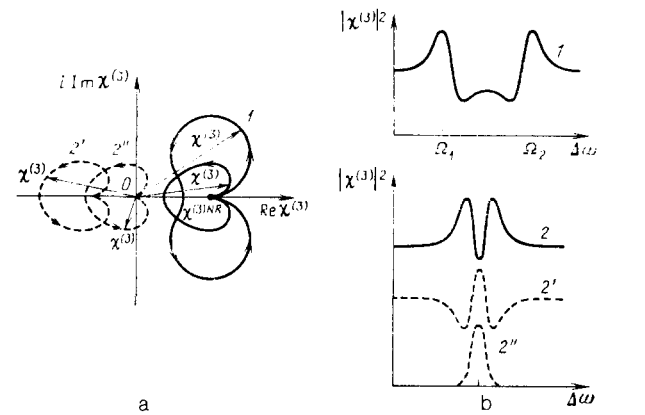

FIG. 5. a—Diagrams in the complex plane of $\chi^{(3)}(\Delta\omega) = \mathrm{Re}\,\chi^{(3)} + i\,\mathrm{Im}\,\chi^{(3)}$ explaining the principle of resolution of a doublet of superposed lines in amplitude-polarization CARS; 1—the $\chi^{(3)}(\Delta\omega)$ relationship for two separated ($|\Omega_1 - \Omega_2| > 2\Gamma$) interfering resonances of Lorentzian form having opposite signs of the peak value of the contribution $\bar{\chi}^{(3)\mathrm{R}}$ to $\chi^{(3)}$; 2 (closed curve on the right in Fig. a), 2′, 2″—the same for close-lying resonances not resolvable by the Rayleigh criterion ($|\Omega_1 - \Omega_2| < \Gamma$, where Γ is the half-width of either of the interfering resonances) for different values of the nonresonance contribution $\chi^{(3)\mathrm{NR}}$ to $\chi^{(3)}$. b—Dispersion curves of $|\chi^{(3)}(\Delta\omega)|^2 \propto I_a(\Delta\omega)$ corresponding to curves 1 and 2 in Fig. a.

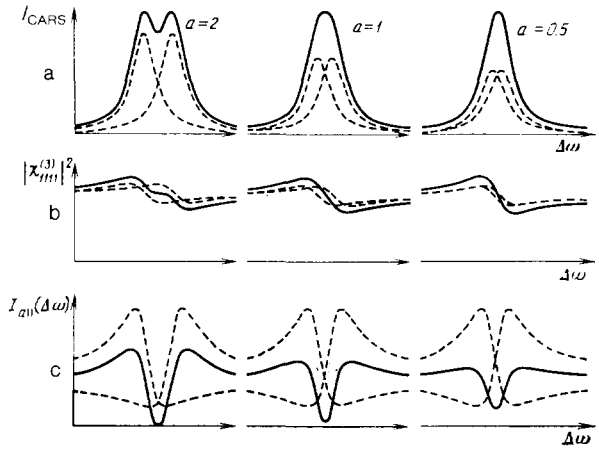

FIG. 6. Pattern of the superposition of a pair of lines of identical intensity, form (Lorentzian), and width (2Γ): in spontaneous Raman spectra (a), in the ordinary scheme of amplitude CARS with measurement of the disperison of $|\chi_{1111}(\Delta\omega)|^2$ (b), and in amplitude-polarization CARS (c). The parameter of the curves is the relative distance between the centers of the lines $a = |\Omega_1 - \Omega_2|/\Gamma$. Solid lines—resulting curves; dotted lines—individual contributions of each of the lines ($\varepsilon = 0.14°$, $\rho_1 = 0.33$, $\rho_2 = 0.35$, $\bar{\chi}^{(3)R}_{1111}/\chi^{(3)NR}_{1111} = 0.1$).

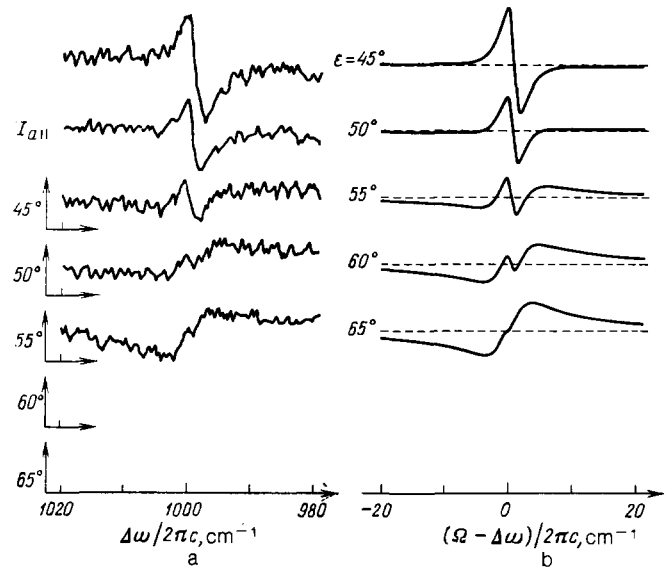

FIG. 7. a—Amplitude-polarization CARS spectra of the line $\Omega/2\pi c = 1000\ \text{cm}^{-1}$ of pure liquid styrene $I_{a\|}(\Delta\omega)$ demonstrating the presence in it of a degenerate doublet structure[14]; as we see, at no orientation of the polarizing anlayzer (given by the angle ε) can one obtain a nondispersing signal $I_{a\|}(\Delta\omega) = \text{const}$ characteristic of a completely "suppressed" isolated line; in the experiment of Ref. 14 the angle φ between the pump polarization unit vectors $\mathbf{e}_1$ and $\mathbf{e}_2$ was chosen close to 90° ($\varphi = 85°$) so as to equalize the relative "strengths" $\alpha_{1,2}$ of the two components (polarized, $\rho = 0$, and depolarized, $\rho = 0.75$) of the line being studied. b—Calculated $I_{a\|}(\Delta\omega)$ relationships corresponding to the experimental curves.

qualitatively. Thus, in the case being studied, two arbitrarily close lines, by interfering, will always be resolved in amplitude-polarization CARS spectra.

To illustrate, Fig. 6 shows the calculated patterns of superposition of two isolated Raman lines of Lorentzian shape having identical widths, identical peak values of the components $\bar{\chi}^{(3)R\sigma}_{1111}$ (i.e., identical spontaneous Raman cross sections), but with slightly different polarization characteristics $\rho_\sigma = \chi^{(3)R\sigma}_{1212}/\chi^{(3)R\sigma}_{1111}$ (i.e., degrees of depolarization in the spontaneous Raman spectra): $\rho_1 = 0.33$, $\rho_2 = 0.35$—in the spontaneous Raman spectra (a), in the ordinary (amplitude) variant of CARS without special choice of the recording conditions (b), and in amplitude-polarization CARS with a specially chosen phase and amplitude of the coherent background (c).[29] As we see from Fig. 6, in AP CARS the spectral doublet is distinctly resolvable even when the centers of the lines have approached to a distance half as large as the half-width of each of the components, i.e., four times as close as the minimal distance at which these lines can be resolved by the Rayleigh criterion in the traditional forms of spectroscopy not employing the principle of spectral holography.

At present this feature of AP CARS (just like coherent Raman ellipsometry—see below), which was first noted in Refs. 2 and experimentally realized in Refs. 3 and 4, is widely employed in spectroscopy to resolve close-lying and merged lines.[8-15]

Figure 7 shows how it has been possible with the aid of AP CARS to resolve a pair of lines of Lorentzian shape that are fully degenerate in frequency ($\Omega_1 = \Omega_2$), but have a different width ($\Gamma_1/2\pi c = 1.4\ \text{cm}^{-1}$, $\Gamma_2/2\pi c = 2.5\ \text{cm}^{-1}$) and degree of polarization ($\rho_1 = 0$, $\rho_2 = 0.75$). (In the experiment of Ref. 14 a study was actually made of the completely symmetric Raman line at the frequency $\Omega/2\pi c = 1000\ \text{cm}^{-1}$ of pure styrene, which has both isotropic ($\rho_1 = 0$) and anisotropic ($\rho_2 = 0.75$) components superposed on one another.

In a recently performed experiment,[8] AP CARS was applied for studying the rotational isomers of conformer molecules in a liquid. The vibrational spectra of such molecules often look completely identical. In the study it was possible for the first time to distinguish spectroscopically the two rotational isomers of 1,2-dichloroethane by analyzing the structure of the band $\Omega/2\pi c = 1306\ \text{cm}^{-1}$. In spontaneous Raman scattering the latter looks like a single, symmetrical line with the half-width $\Gamma/2\pi c = 7\ \text{cm}^{-1}$ and degree of polarization $\rho = 0.3$. However, CARS reveals the doublet structure of this band. Figure 8 shows the results of an experiment[8] (points 1) for several positions of the polarizer given by the angle ε and the contours calculated by Eqs. (29) and (30) of the spectral curves $I_{a\|}(\Delta\omega)$ (solid curves 2) under the assumption that the line being studied is formed by superposition of a pair of close-lying resonances with the half-widths $\Gamma_1/2\pi c = \Gamma_2/2\pi c = 6\ \text{cm}^{-1}$, degrees of depolarization $\rho_1 = 0.05$ and $\rho_2 = 0.6$, and differing intensities: $\alpha_1 = 0.2$, $\alpha_2 = 0.1$, and with $(\Omega_1 - \Omega_2)/\Gamma_1 = 1$. The dotted line 3 in this same diagram shows the course of the spectral contour of the relationship $I_{a\|}(\Delta\omega)$ calculated under the assumption of existence of a single resonance having the parameters of the spontaneous Raman line.

Another characteristic example of effective conformational analysis of a liquid (n-pentane) using amplitude-polarization active Raman spectroscopy is shown in Fig. 9[11,30] (see also Fig. 2). In the liquid state n-pentane exists in the form of three rotational isomers: trans–trans (TT), trans–gauche (TG) and gauche–gauche (GG). However, it has not been possible spectroscopically to detect the difference of the TT- and TG-isomers in the band at $\sim 870\ \text{cm}^{-1}$. Fig-

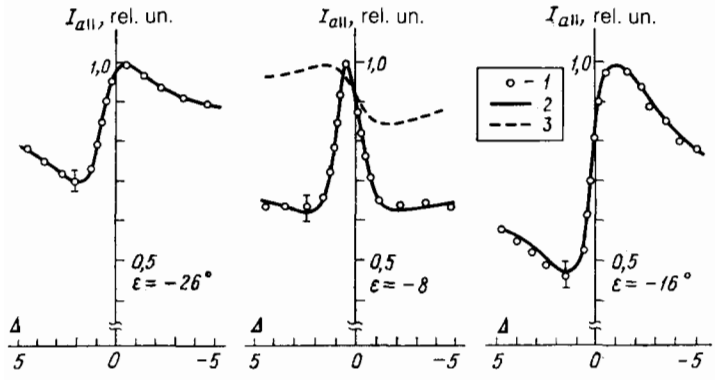

FIG. 8. Amplitude-polarization CARS spectra of the line $\Omega/2\pi c = 1306$ cm^{-1} of liquid dichloroethane[8]: 1—experiment; 2—calculation assuming a doublet structure of the line; 3—calculation assuming a singlet structure. The angles ε_1 (left) and ε_2 (right) correspond to the position of the polarizer crossed with the polarization direction of the first ($\mathbf{P}^{R_1}$) and second ($\mathbf{P}^{R_2}$) resonance contributions to $\mathbf{P}^{(3)}$, respectively, $\Delta = (\omega_1 - \omega_2 - \Omega_1)/\Gamma_1$ is the normalized detuning from the center of one of the lines, and $\Gamma_1/2\pi c = 3$ cm^{-1}.

ure 9a shows the polarized (1) and depolarized (2) spontaneous Raman spectra of the line $\Omega/2\pi c \approx 870$ cm^{-1} belonging to the deformational vibrations of the CH_3 groups of the TT- and TG-isomers. As we see, the complex character of this line is manifested only in the form of a weakly marked low-frequency tail of the spontaneous Raman line.

Yet, by choosing the polarization conditions for recording in AP CARS, one can completely resolve the doublet structure of this band (Fig. 9b) and trace the temperature dependence of the relative intensity of the lines corresponding to the TT- and TG-isomers, and thus determine the difference in enthalpies of these conformers of *n*-pentane (in this case 600 ± 200 cal/mole). Table I gives the parameters of the resonances determined from AP spectra that correspond to the stated two rotational isomers for different tempertures. Just like the examples given above, these data indicate the attainment of a spectral resolution considerably exceeding the limiting resolution for the ordinary types of spectroscopy as established by the Rayleigh criterion.

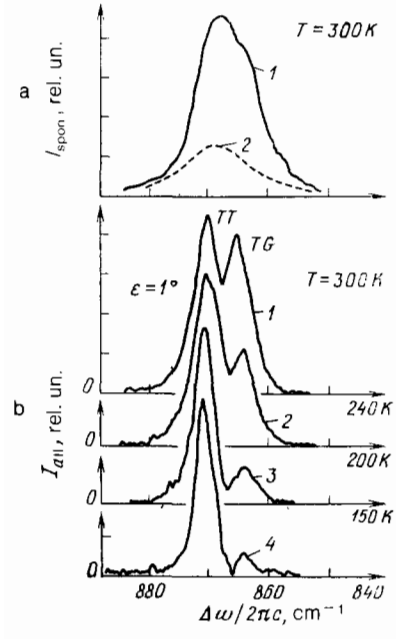

FIG. 9. a—Sponaneous Raman spectrum of liquid *n*-pentane at $T = 300$ K; 1—polarized, not showing the splitting caused by the two rotational isomers TT and TG of the molecules of the liquid. b— AP CARS spectra of liquid *n*-pentane at different temperatures demonstrating the interference of the two close lines corresponding to vibrations of the different conformers (the angle $\varepsilon = 1°$ for all the curves 1–4).

The high sensitivity of the polarization variants of CARS to small variations of frequencies and polarization characteristics in conformer molecules opens up extremely interesting prospects for applying coherent spectroscopy for studying proteins and nucleic acids, in which precisely the conformational changes characterize the different degrees of their biological activity. Figure 10 shows the polarization CARS spectrum of a protein (a solution of α-chymotrypsin in water) obtained with almost complete suppression of the nonresonance CARS signal from water[13] (see also Ref. 56). Here one can already see distinctly the presence of a number of individual components interfering with one another under the overall spectral contour that is not resolved in spontaneous Raman scattering.

5. RESOLUTION OF THE INTERNAL STRUCTURE OF BROAD SCATTERING AND ABSORPTION BANDS BY THE METHOD OF HOLOGRAPHIC SPECTROSCOPY. MULTIDIMENSIONAL SPECTROSCOPY

After analyzing in detail the very simple, though crucial problem of contrast-rich resolution of a pair of close-lying lines by using the polarization variants of CARS, we arrived at the end of the preceding section at the more general problem of resolving the internal structure of broad, superposed spectral bands and extracting complete spectral information about a scattering (or absorbing) medium by the methods of holographic spectroscopy.

To analyze this situation, it is of interest to turn to the panoramic polarization CARS spectra and coherent Raman ellipsometry encompassing extended regions of the dispersion curves $I_{a\parallel}(\Delta\omega)$, $I_{a\perp}(\Delta\omega)$, and their ratio.

Figure 11 shows several such CRE spectra of benzene in the range 2900–3200 cm^{-1} (dots).[31] The variation of the orientation of the polarizing prism given by the angle ε leads to a cardinal change in the overall form of these spectra.

Of course, in line with what we have said in Secs. 1, 3, and 4, these spectral curves that little resemble one another have common invariants that reduce to the real and imaginary parts of the cubic susceptibility tensor: $\chi^{(3)}_{1122}(\Delta\omega)$, $\chi^{(3)}_{1212}(\Delta\omega)$, and $\chi^{(3)}_{1221}(\Delta\omega)$. The overall form of the CRE spectra in Fig. 11 is described by Eq. (32), and hence is a coherent superposition of a number of optical resonances that represent in this case different eigenvibrations and overtones of the benzene molecule.

The solid lines drawn through the experimental points in Fig. 11 were derived by Eq. (32) with the appropriate values of the angle ε and by using the parameters of the indi-

TABLE I. Parameters of the vibrational resonances of the TT- and TG-isomers of *n*-pentane in the region of 870 cm^{-1} measured by using amplitude-polarization active Raman spectroscopy.

	Ω_1 *). TT		Ω_2 *), TG	
Degree of polarization ρ_σ	0.15±0.03		0.05±0.05	
Parameters of lines	$\frac{\chi^{(3)}_{1111}R}{\chi^{(3)}_{1111}NR}$	$\frac{2\Gamma}{2\pi c}$, cm^{-1}	$\frac{\chi^{(3)}_{1111}R}{\chi^{(3)}_{1111}NR}$	$\frac{2\Gamma}{2\pi c}$, cm^{-1}
300 K	0.4±0.1	8.1±0.3	0.15±0.02	5.2±0.3
240 K	0.6±0.2	4.4±0.3	0.12±0.03	2.8±0.3
200 K	0.8±0.2	3.9±0.3	0.15±0.03	3.1±0.3
150 K	1.2±0.3	3.1±0.3	0.17±0.04	2.5±0.3

*) $(\Omega_1 - \Omega_2)/2\pi c = 4 \pm 1$ cm^{-1}.

vidual resonances in Lorenzian form given in Table II. Despite individual small discrepancies, on the whole the set of calculated spectra describes the experimental spectra well. It is important to stress that the determination of the parameters of weak scattering lines corresponding to the overtones of molecular vibrations has become possible here owing to their interference in the CRE spectra with the coherent background and with the more intense first-order scattering bands. In ordinary Raman spectra it is practically impossible to measure their parameters exactly, precisely because of closeness to the stronger first-order lines.

The fact is also very significant that in polarization CARS the experimenter obtains not one or two projections, as in the traditional forms of spectroscopy, but an arbitrarily large number of different "projections" of the spectra of the same set of optical resonances. This enables one to pose and solve the *inverse spectroscopic problem* with a substantially larger degree of error than in spontaneous Raman spectroscopy.[32-34] One can interpret the change in the conditions of recording spectra in polarization active spectroscopy as a change in the "vantage point" of the experimenter toward the set of optical resonances of interest to him or as obtaining different two-dimensional cross sections of a certain six-dimensional manifold fixed by the set of six functions of the frequency detuning $\Delta\omega$: the real and imaginary parts of the three independent components of the cubic optical susceptibility of the homogeneous, isotropic nonabsorbing liquid, $\chi^{(3)}_{1122}(\Delta\omega)$, $\chi^{(3)}_{1212}(\Delta\omega)$, and $\chi^{(3)}_{1221}(\Delta\omega)$.

Figure 12 shows an example of a panoramic CRE spectrum of water at room temperature.

The coherent Raman ellipsometry spectra of the band of stretching OH vibrations of water for different ε values distinctly indicate the complex intereference character of this anomalously broad band. However, under no conditions does clear resolution of its individual components arise. Nevertheless, the data of coherent spectroscopy prove substantially more information-rich and senstive to the details of the inner structure of this band, and also to the tempera-

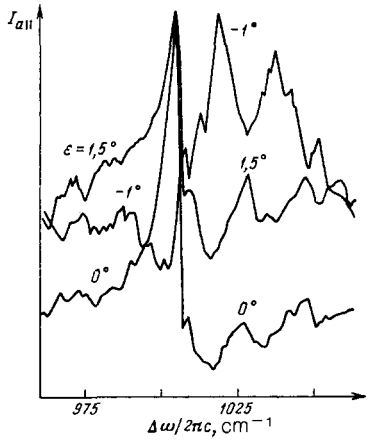

FIG. 10. Amplitude-polarization CARS spectra of an aqueous solution of the protein α-chymotrypsin showing the complex internal structure of the band ~1020 cm^{-1} (according to Ref. 13).

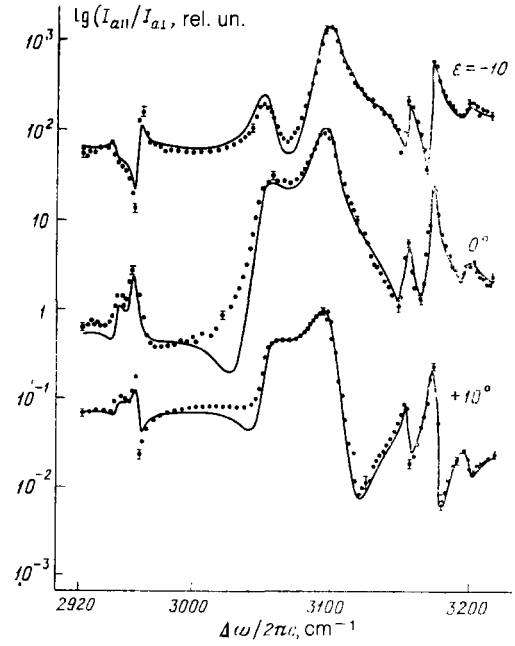

FIG. 11. Panoramic coherent Raman ellipsometry (CRE) spectra of liquid benzene $I_{a\parallel}(\Delta\omega)/I_{a\perp}(\Delta\omega)$ at $T = 300$ K in the range $\Delta\omega/2\pi c = 2900$–$3200$ cm^{-1} for several values of the angle ε. Dots—experiment; solid lines—calculation using the data of Table II.[31] The dispersion curves have been arbitrarily displaced with respect to one another along the axis of ordinates.

TABLE II. Spectroscopic parameters of the stretching CH vibration bands of benzene determined by CRE[31].

$\frac{\Omega_\sigma}{2\pi c}$, cm^{-1}	Assignment	$\frac{\bar{\chi}^{(3)}_{1111}}{\chi^{(3)NR}_{1111}}$	$\frac{\chi^{(3)}_{1212}}{\bar{\chi}^{(3)}_{1111}}$	$\frac{\Gamma_\sigma}{2\pi c}$, cm^{-1}	$\frac{\Omega_\sigma}{2\pi c}$, cm^{-1}	Assignment	$\frac{\bar{\chi}^{(3)}_{1111}}{\chi^{(3)NR}_{1111}}$	$\frac{\chi^{(3)}_{1212}}{\bar{\chi}^{(3)}_{1111}}$	$\frac{\Gamma_\sigma}{2\pi c}$, cm^{-1}
2940	$\nu_3+\nu_{16}$	0.1	0.7	2	3160	$2\nu_{16}$	0.5	0.2	2
2955	$\nu_2+\nu_3+\nu_{18}$	0.8	0.1	1	3178	$\nu_2+\nu_6+\nu_{18}$	0.6	0.1	2
3045	ν_{15}	2.2	0.5	7	3205	$2(\nu_2+\nu_{18})$	0.1	0.1	3
3068	ν_1	3.0	0.1	8					

ture, salinity, and presence of impurities than the data of spontaneous Raman scattering.[10]

It has not yet been possible to obtain a complete solution of the inverse spectral problem of active Raman spectroscopy as applied to the stated Raman band of water (i.e., it has not been possible to use the experimental CRE dispersion curves to find the final set of parameters of the individual resonances Ω_σ, Γ_σ, ρ_σ and $\chi^{(3)R\sigma}_{1111}/\bar{\chi}^{(3)NR}_{1111}$ that give rise to this band on superposition and fully reproduce the course of all the experimental curves). However, one can subject to direct test a set of "models" of this band[5,29,31] proposed at various times by Schultz and Hornig,[35] Murphy and Bernstein,[36], Walrafen,[37] Scherer *et al.*,[38] etc. Until recently the fundamental criterion of the correctness of the concepts on which some model of liquid water was based (just as for other liquids) was agreement of the predictions yielded by the models with the form and character of the spontaneous Raman and infrared absorption spectra.[35–38] Despite the considerable difference of the stated models among themselves, they all practically completely reproduce the spontaneous Raman and infrared absorption spectra. However, in polarization CARS (CRE) the differences between these models are extremely sharply manifested.[5,29,31] For the models of Schultz and Hornig and of Walrafen, one cannot obtain even qualitative agreement of the predicted CRE spectra with those experimentally observed; the models of Murphy and of Scherer allow obtaining qualitative agreement, but yield crude quantitative discrepancies among themselves and with the experimental dispersion curves. The calculated spectra are very sensitve to the phase and amplitude of the coherent background.

Especially varied potentialities of observing interference phenomena exist in resonance active Raman spectroscopy, i.e., in the presence in the Raman-active medium being studied of single-photon absorption at one or several of the frequencies ω, ω_1, and ω_2 that participate in exciting the anti-Stokes signal: $\omega_a = \omega + \omega_1 - \omega_2$.

In terms of the nonlinear optical susceptibilities, this situation is described as the appearance of imaginary parts of the components of the electronic susceptibilities (previously termed nonresonance) $\chi^{(3)E}_{jkl}$ and also of the quantities $\bar{\chi}^{(3)R}_{ijkl}$, and the appearance of deviations in the relationships among the independent components of this tensor from the Kleinman relationships of (10). Under these conditions the interference of the electronic and Raman resonances acquires an especially capricious character so that, in particular, the potentialities are even more expanded for resolving the internal structure of superposed scattering bands (Figs. 13, 14).

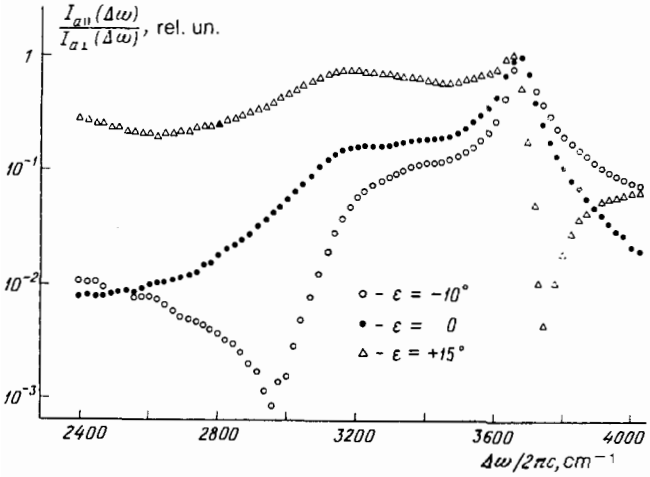

FIG. 12. CRE spectra $I_{a\parallel}(\Delta\omega)/I_{a\perp}(\Delta\omega)$ of water at $T \approx 300$ K for different values of the angle ε, demonstrating the complex internal structure of this Raman band.

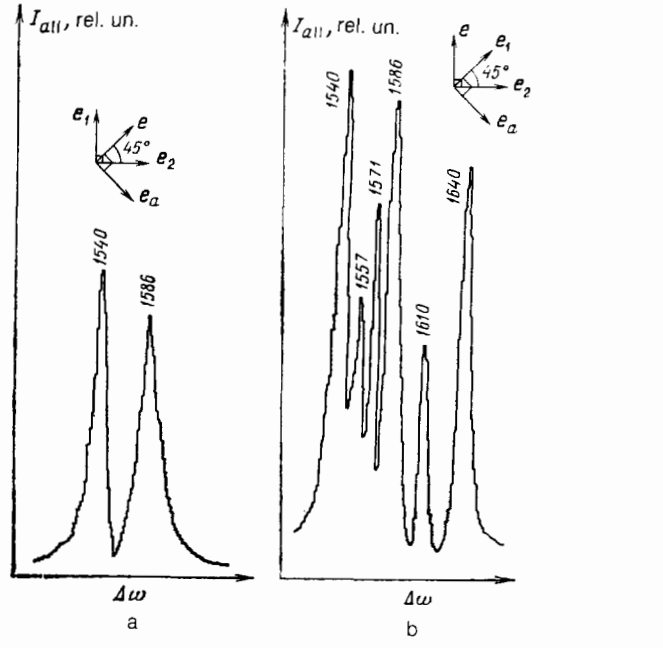

FIG. 13. Amplitude-polarization resonance CARS spectra with nondegenerate frequencies in a solution of copper octaethylporphyrin in tetrahydrofuran with different mutual orientations of the polarization vectors of the interacting waves (diagrams shown[12,28] with the corresponding spectra in Figs. a and b). Control of the polarization in the AP scheme of resonance CARS enables measuring all the polarization parameters of close-lying and superposed lines corresponding to vibrations of differing symmetry, not only in the ground state, but also in an excited electronic state.

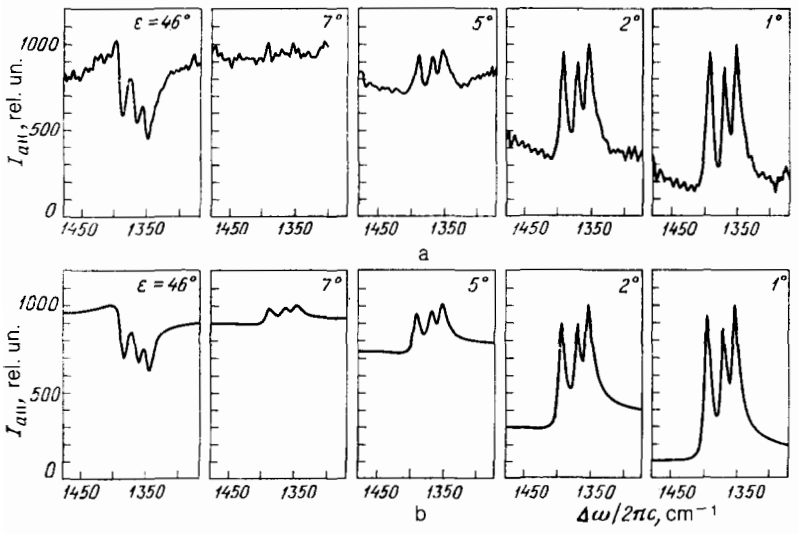

FIG. 14. Complex structure of a group of resonance Raman lines of a solution of pseudoisocyanine chloride in water resolved by using AP CARS. a—Experiment, b—calculation[15] ($\varphi = 72°$, $\lambda_1 = 563.9$ nm).

An essential difference between resonance CARS (and active Raman spectroscopy in general) and resonance Raman scattering is that the interference phenomena in coherent spectroscopy characteristic of resonance scattering arise even when certain molecules of a solution or gas mixture are responsible for light absorption, but others for Raman scattering.[6,40,41] The reason for this is the coherence of the scattering, which is expressed, in particular, in the addition of the resonance nonlinear susceptibilities of the molecules of different types that undergo resonance of the electronic ($\chi^{(3)E}$) and Raman ($\chi^{(3)R}$) types:

$$\chi^{(3)}_{\text{mixt}} = \chi^{(3)NR} + \chi^{(3)E}_{\text{abs}} + \chi^{(3)R}_{\text{Raman}},$$

and in the existence in the measured intensity of a cross-term (the fourth term on the right-hand side):

$$\frac{I_a(\omega_a)}{II_1I_2} \sim |\chi^{(3)}|^2 = |\chi^{(3)NR}|^2 + |\chi^{(3)E}|^2 + |\chi^{(3)R}|^2 + 2\,\mathrm{Re}\,(\chi^{(3)E*}\chi^{(3)R}) + 2\,\mathrm{Re}\,(\chi^{(3)NR}\chi^{(3)R}) + 2\,\mathrm{Re}\,(\chi^{(3)NR}\chi^{(3)E}). \quad (33)$$

Much new information that is lacking in principle in the data of traditional single-photon absorption spectroscopy is contained in the spectra of coherent anti-Stokes (or Stokes) light scattering of absorbing media lacking Raman resonances, while one of the frequencies ω, ω_1, or ω_2 is scanned over a single-photon absorption band.[42–45] One can show (see Refs. 6 and 44) that in this case the observed active spectra $I_a(\omega_a)$, where $\omega_a = \omega + \omega_1 - \omega_2$, and, e.g., ω_2 is scanned, are the result of interference of two closely coupled coherent processes of single-photon absorption and hyper-Raman scattering by the electronic transition being studied. Figure 15 shows the coherent ellipsometry spectrum of an absorbing medium (a solution of neodymium nitrate in water) that demonstrates the resolved triplet structure (involving the Stark splitting of the electronic states of the hydrated Nd^{3+} ions; see Ref. 45), which is practically completely lacking in the single-photon absorption spectrum.

Here we encounter anew the extraction from coherent scattering spectra of substantially more complete information on the electronic resonance being studied than that contained in the data of traditional noncoherent spectroscopy—in this case, single-photon absorption.

6. CONCLUSION

Let us summarize the discussion that we have conducted. The shift to recording the coherent response of the medium under study to a multifrequency optical agent enables a cardinal increase in the information content of the obtained spectroscopic data. The interference nature of the coherent light-scattering spectra allows one to realize the extraction of *complete* spectroscopic information on the medium under study (in this case, contained in the dispersion curves of the real and imaginary parts of the independent components of the cubic optical susceptibility tensor), and thus to solve the

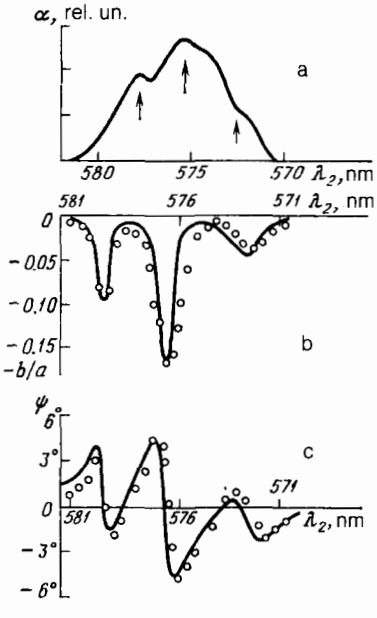

FIG. 15. Dispersion of the elliptic-polarization parameters of the anti-Stokes signal ($\omega_a = 2\omega_1 - \omega_2$) generated in a solution of neodymium nitrate in water as the frequency ω_2 is scanned (wavelength $\lambda_2 = 2\pi c/\omega_2$) over the absorption line of Nd^{3+} ions at 571–581 nm. a—Shape of the line of the absorption coefficient $\alpha(\lambda_2)$; the arrows indicate the features of the absorption spectrum that are manifested in the CRE spectrum in the form of individual components. b—Dispersion of the ratio b/a of the small b to the large a axis of the ellipse of polarization of the anti-Stokes signal; the minus sign corresponds to rotation of the ellipse of polarization in the negative direction. c—Dispersion of the angle ψ of inclination of the great axis of the ellipse.[43,45] Circles—experiments, lines—calculation.

phase problem in optical spectroscopy. In many ways this is analogous to how the interference of the reference wave with the diffraction field of the wave from the object of study in optical holography enables one to carry out the recording of complete information on this object, and thus to solve the optical phase problems. To speak in radiophysical language, coherent active spectroscopy enables one to carry out optical heterodyning of the spectrum being recorded.[46] Unfortunately, one cannot fully draw the analogy with optical holography in coherent nonlinear spectroscopy, since the extraction of the complete information contained in the coherent spectra about the optical resonances of the medium being studied involves a systematic controlled variation of the interference of the information-bearing components of the frequency spectrum with one another and with the coherent background in recording the spectra and solving the inverse spectral problem on this basis. Yet in holography the complete reconstruction of the image of the object occurs "automatically" in the diffraction by the interference pattern written in the photosensitive recording medium by the readout wave (which coincides with the reference wave in the method of D. Gabor and is "automatically" selected by the recording medium in the method of Yu. N. Denisyuk[7]).

This situation distinguishes the *holographic spectroscopy* described in this article from the recently developed methods of dynamic *spectral holography*,[47-50] which completely realize the holographic principle of recording and readout of information about the amplitudes and phases of spectral components of nonstationary light fields upon interference in a photosensitive medium of signal and reference pulses. Of course, the purposes and initial premises of holographic spectroscopy and spectral holography also differ.

In coherent active spectroscopy the physical information on the medium being studied is multidimensional even in the simplest case of an isotropic, homogeneous, transparent medium. The spectra obtained in the polarization variants of active spectroscopy of such media, e.g., the $I_{a\parallel}(\Delta\omega)$ relationship in amplitude-polarization CARS, amount to apparent two-dimensional cross sections of a six-dimensional manifold that represents the optical references under study by using six independent real functions of the frequency detuning $\Delta\omega$:

$$\operatorname{Im}\chi^{(3)}_{1122}(\Delta\omega),\quad \operatorname{Re}\chi^{(3)}_{1122}(\Delta\omega),\quad \operatorname{Im}\chi^{(3)}_{1212}(\Delta\omega),\quad \operatorname{Re}\chi^{(3)}_{1212}(\Delta\omega),$$
$$\operatorname{Im}\chi^{(3)}_{1221}(\Delta\omega),\quad \operatorname{Re}\chi^{(3)}_{1221}(\Delta\omega).$$

In isotropic media having one- and two-photon absorption resonances, and also in crystals in the presence of external static fields and mechanical stresses, etc., the number of independent components of the tensor $\chi^{(3)}_{ijkl}$ and their frequency arguments increases even further. The controlled change in the conditions of recording spectra in active spectroscopy is equivalent to changing the angle of vision of the experimenter toward the resonance being studied. This allows one to obtain complete information on it, including the selection of the most convenient vantage point at which the hidden details of the spectrum are manifested in greatest contrast. Precisely this constitutes the activity of coherent spectroscopy, whereas the character of the way that the spectra are taken remains unperturbing; the probe electric field exerts no real distorting action on the resonances being studied in the material (as happens in the above-cited spectroscopy of absorption saturation[5] or in the spectroscopy of "trough burning"[51]).

In evaluating the comprehensiveness and completeness of the spectroscopic information in coherent polarization spectroscopy, it is expedient to discuss the problem of the degree of independence of the data extracted from the dispersion curves of the imaginary and real parts of the nonlinear susceptibilities. As is known, in linear optics the universal Kramers-Kronig[57] dispersion relationship exists between the real and imaginary parts of the complex dielectric permittivity of the medium. In nonlinear optics analogous general relationships exist between the imaginary and real parts of the nonlinear susceptibilities. However, as N. Bloembergen[21] has noted (see also Refs. 58 and 59), the usefulness of these relationships is often very limited. Nevertheless, in the cases in which the Born-Oppenheimer approximation holds and, correspondingly, the cubic susceptibilities that figure in active Raman spectroscopy prove to be functions of a single argument—the pump frequency difference $\Delta\omega=\omega_1-\omega_2$, the representation (4) is valid for the nonlinear susceptibilities. The real and imaginary parts of the resonance Raman susceptibility $\chi^{(3)R}_{ijkl}(\Delta\omega)$ prove to be coupled by integral relationships that are direct analogs of the Kramers-Kronig dispersion relationships[60]:

$$\operatorname{Re}\chi^{(3)R}_{ijkl}(\Delta\omega)=-\frac{1}{\pi}\int_0^\infty d\omega'\,\operatorname{Im}\chi^{(3)R}_{ijkl}(\omega')\,(\omega'-\Delta\omega)^{-1},$$
$$\operatorname{Im}\chi^{(3)R}_{ijkl}(\Delta\omega)=\frac{1}{\pi}\int_0^\infty d\omega'\,\operatorname{Re}\chi^{(3)R}_{ijkl}(\omega')\,(\omega'-\Delta\omega)^{-1}. \tag{34}$$

The integrals are taken as the principal value throughout the frequency band occupied by the Raman resonances. In agreement with Eqs. (11) within the framework of this same adiabatic approximation, a fluctuation-dissipation theorem holds, which relates the contours of the polarized, depolarized, and inverted incoherent Stokes components observed in spontaneous Raman scattering to the dispersion curves of the imaginary parts of the corresponding elements of the resonance Raman cubic susceptibility tensor.

This means that, if one measures the complete dispersion curves of $\operatorname{Im}\chi^{(3)B}_{ijkl}(\Delta\omega)$ by using incoherent spontaneous Raman spectroscopy and employs (34), one can in principle reconstruct also the complete dispersion curves of $\operatorname{Re}\chi^{(3)B}_{ijkl}$. However, in practice, far from always can these possibilities in principle be realized—as a rule, only for isolated Raman lines or for groups of isolated Raman lines, i.e., precisely in the cases in which the data of the noncoherent Raman methods quite suffice for complete solution of the inverse spectral problem.

The heuristic role of the relationships of the Kramers-Kronig type of (34) is sharply diminished in the more complex cases of superposed lines, of incomplete information on the form of the spontaneous Raman spectrum over the entire scale of frequencies $\Delta\omega$, of high noise level in the spectra being recorded, and also, of course, in the presence of one- or two-photon absorption at one or several frequencies used for taking the spontaneous Raman spectra. Thus the potentiality of directly obtaining complete information on the medium from the data of polarization coherent spectroscopy proves highly valuable.

Here one must bear in mind the fact that it is generally impossible to measure the magnitudes and signs of the electronic nonlinear susceptibilites $\chi_{ijkl}^{(3)NR}$ by using spontaneous Raman scattering in homogeneous, isotropic, transparent media. To do this, the only methods proving suitable are those of coherent nonlinear spectroscopy.

These same methods, as was noted in Sec. 5, make it possible to obtain fundamentally new information on the resonance electronic susceptibilities of absorbing media. In particular, the data of coherent active spectroscopy contain information not only on the dipole moments and shape of the resonance line of an electronic transition, as do the data of noncoherent linear absorption spectroscopy, but also the components of the hyper-Raman scattering tensor for the electronic transition being studied.[6,44] The information on the parameters of electronic transitions extractable from the spectra of coherent active spectroscopy inside an absorption line proves even more varied and complete (i.e., when all four frequencies that participate in the nonlinear interaction lie within the contour of an absorption line of the absorbing medium) (Ref. 6, Chap. 7).[61,62]

At the same time, we must bear in mind the limitations in principle of the methods of coherent four-photon spectroscopy in resolving the internal structure of inhomogeneously broadened lines, in particular, Doppler-broadened lines of light scattering and absorption in gases and plasmas. The fine structure of such lines that is concealed by Doppler broadening cannot be revealed here by the methods of coherent spectroscopy. To extract it requires supplementing the coherent four-photon methods with the methods of saturation spectroscopy. Examples of such a generalization of the coherent methods are contained in Refs. 63–67.

To summarize, we should conclude that polarization coherent active spectroscopy of light scattering and absorption, which is based on using four-photon interactions, constitutes a highly information-rich form of holographic multidimensional spectroscopy that substantially expands the potentialities of the optical methods of studying matter. The use of the additional information extractable from coherent active spectra is most productive in the problems in which application of the traditional noncoherent spectroscopic methods faces difficulties in interpreting the obtained data owing to insufficient spectral resolution, ambiguity, and false solution of the inverse spectral problem, etc.

The author is deeply grateful to S. A. Akhmanov for the idea of writing this article, and for support of many years and discussion of the problems treated here, as well as to his colleagues and associates for aid and friendly participation.

[1)]N. Bloembergen[52] has also pointed out the great similarity between nonlinear optical phenomena and holography. In current studies this situation is employed, in particular, for applying the well-developed mathematical methods of nonlinear optics to solve electrodynamic problems in holography; see, e.g., Ref. 53.

[2)]In the scheme of coherent Raman spectroscopy with degenerate frequencies, i.e., with $\omega = \omega_1$, $\omega_a = 2\omega_1 - \omega_2$, the number of independent components of the tensor $\chi_{ijkl}^{(3)}(\Delta\omega)$ is reduced to two.

[1]S. A. Akhmanov and N. I. Koroteev, Usp. Fiz. Nauk **123**, 405 (1977) [Sov. Phys. Usp. **20**, 899 (1977)].
[2]S. A. Akhmanov, A. F. Bunkin, S. G. Ivanov, and N. I. Koroteev, Pis'ma Zh. Eksp. Teor. Fiz. **25**, 444 (1977) [JETP Lett. **25**, 416 (1977); A. F. Bunkin, M. G. Karimov, and N. I. Koroteev, Vestn. Mosk. Univ. Fiz. Astron., Ser. 3, **19**, 3 (1978); N. I. Koroteev, J. Opt. Soc. Am. **68**, 1432 (1978).
[3]L. S. Aslanyan, A. F. Bunkin, and N. I. Koroteev, Opt. Spektrosk. **46**, 165 (1979) [Opt. Spectrosc. (USSR) **46**, 89 (1979)].
[4]N. I. Koroteev, M. Endemann, and R. L. Byer, Phys. Rev. Lett. **43**, 398 (1979).
[5]V. S. Letokhov and V. P. Chebotaev, *Nonlinear Laser Spectroscopy*, Springer Verlag, Berlin (1977) [Russ. original, Nauka, M., 1975].
[6]S. A. Akhmanov and N. I. Koroteev, Methods of Nonlinear Optics in Light-Scattering Spectroscopy (in Russian), Nauka, M., 1981.
[7]Yu. N. Denisyuk, ed., Problems of Optical Holography (in Russian), Nauka, L., 1981; L. M. Soroko, *Holography and Coherent Optics*, Plenum Press, New York (1980) (Russ. original, Nauka, M., 1971).
[8]M. F. Vigasina, A. A. Ivanov, R. Yu. Orlov, A. B. Remizov, an A. I. Fishman, Dokl. Akad. Nauk SSSR **283**, 1394 (1985) [Dokl. Phys. Chem. (1985)].
[9]A. F. Bunkin, D. V. Vlasov, A. S. Galumyan, D. V. Mal'tsev, and K. O. Surskiĭ, Kvantovaya Elektron. (Moscow) **12**, 788 (1985) [Sov. J. Quantum Electron. **15**, 513 (1985)].
[10]A. F. Bunkin, D. V. Vlasov, A. S. Galumyan, and K. O. Surskiĭ, Opt. Spektrosk. **58**, 481 (1985) [Opt. Spectrosc. (USSR) **58**, 289 (1985)].
[11]A. A. Ivanov, R. Yu. Orlov, and A. I. Fishman, in Abstracts of Reports of the 12th All-Union Conference on Coherent and Nonlinear Optics (in Russian), Moscow, 1985, Vol. 1, p. 197.
[12]P. A. Apanasevich, V. V. Kvach, V. P. Kozich, and V. A. Orlovich (in Russian), Preprint No. 381 of the Institute of Physics, Academy of Sciences of the Belorussian SSR, Minsk, 1985.
[13]V. F. Kamalov, N. I. Koroteev, B. N. Toleutaev, A. Yu. Chikishev, and A. P. Shkurinov, Izv. Akad. Nauk SSSR Ser. Fiz. **50**, 1197 (1986) [Bull. Acad. Sci. USSR Phys. Ser. 50(6), 147 (1986)].
[14]R. Igarashi, F. Iida, C. Hirose, and I. Fujiyma, Bull. Chem. Soc. Jpn. **54**, 3691 (1981).
[15]R. Brakel, V. Mudogo, and F. W. Schneider, J. Chem. Phys. **84**, 2451 (1986).
[16]S. A. Akhmanov and N. I. Koroteev, Zh. Eksp. Teor. Fiz. **67**, 1306 (1974) [Sov. Phys. JETP **40**, 650 (1975)].
[17]M. D. Levenson and N. Bloembergen, Phys. Rev. B **10**, 4447 (1974).
[18]M. D. Levenson, Phys. Today **30**, No. 5, 44 (1977).
[19]A. F. Bunkin, S. G. Ivanov, and N. I. Koroteev, Dokl. Akad. Nauk SSSR **233**, 338 (1977) [Sov. Phys. Dokl. **22**, 146 (1977)]; Pis'ma Zh. Tekh. Fiz. **3**, 450 (1977) [Sov. Tech. Phys. Lett. **3**, 182 (1977)].
[20]C. Flytsanis, in: *Quantum Electronics: a Treatise*, eds. H. Rabin and C. Tang, Academic Press, New York, 1975, Vol. 1, Part A, p. 111.
[21]N. Bloembergen, *Nonlinear Optics*, Benjamin, New York (1965) [Russ. transl., Mir, M., 1966].
[22]A. M. Prokhorov, ed., Handbook of Lasers (in Russian), Sov. radio, M., 1978, Vol. 2, Chap. 41.
[23]Yu. I. Sirotin and M. P. Shaskol'skaya, Fundamentals of Crystal Physics (in Russian), Nauka, M., 1979.
[24]D. A. Kleinman, Phys. Rev. **126**, 1977 (1962).
[25]V. M. Faĭn and É. G. Yashchin, Zh. Eksp. Teor. Fiz. **46**, 695 (1964) [Sov. Phys. JETP **19**, 474 (1964); V. M. Faĭn, Photons and Nonlinear Media (in Russian), Sov. radio, M., 1972, Sec. 14.
[26]S. M. Gladkov and N. I. Koroteev, Kvantovaya Elektron. (Moscow) **9**, 759 (1982) [Sov. J. Quantum Electron. **12**, 469 (1982)].
[27]J. L.Oudar, R. W. Smith, and Y. R. Shen, Appl. Phys. Lett. **34**, 758 (1979).
[28]P. A. Apanasevich, V. V. Kvach, V. P. Kozich, V. A. Orlovich, and A. B. Churkin, Izv. Akad. Nauk SSSR Ser. Fiz. **47**, 1919 (1983) [Bull. Acad. Sci. USSR Phys. Ser. **47**(10), 40 (1983)].
[29]N. I. Koroteev, M. Endemann, and R. L. Byer, *Theory of Light Scattering in Solids*, eds., J. L. Birman, H. Z. Cummins, and K. K. Rebane, Plenum Press, New York, 1979, p. 384.
[30]S. A. Akhmanov, V. F. Kamalov, and N. I. Koroteev, in *Proc. Int. Conference on Light Scattering Spectroscopy of Biological Objects*, Praha, 1986, Elsevier, Amsterdam, 1987.
[31]K. O. Surskiĭ, Polarization Four-Photon Spectroscopy of Broad Raman Bands in a Liquid, Abstract of disseration as candidate in physicomathematical sciences, Physicotechnical Institute, M., 1985.
[32]A. W. Saunders, C. W. Sink, and A. B. Harvey, Appl. Spectroc. **26**, 444 (1972).
[33]J. W. Akitt, *ibid.* **29**, 493 (1975).
[34]P. Gans and J. Gill, *ibid.* **31**, 451 (1977).
[35]I. W. Schultz and F. F. Hornig, J. Phys. Chem. **65**, 2131 (1961).
[36]W. F. Murphy and H. J. Bernstein, J. Chem. Phys. **76**, 1147 (1972).
[37]G. E. Walrafen, in: *Water: a Comprehensive Treatise*, ed. F. Franks, Plenum Press, New York, 1972, Vol. 1, Chap. 5, p. 151.
[38]J. R. Scherer, M. K. Go, and S. Kint, J. Phys. Chem. **78**, 1304 (1974).
[39]P. A. Apanasevich, V. V. Kvach, V. P. Kozich, and V. A. Orlovich, Lasers and Optical Nonlinearity (in Russian), Institute of Physics of the Academy of Sciences of the Belorussian SSR, Minsk, 1986, p. 24.

[40]N. I. Koroteev, Kvantovaya Elektron. (Moscow) **3**, 755 (1976) [Sov. J. Quantum Electron. **6**, 411 (1976)].
[41]A. V. Bunkin, S. G. Ivanov, and N. I. Koroteev, Pis'ma Zh. Eksp. Teor. Fiz. **24**, 468 (1976) [JETP Lett. **24**, 429 (1976)].
[42]S. A. Akhmanov, L. S. Aslanyan, A. F. Bunkin, *et al.*, see Ref. 29, p. 409.
[43]L. S. Aslanyan, A. F. Bunkin, S. M. Gladkov, and S. G. Ivanov, Opt. Spektrosk. **48**, 85 (1980) [Opt. Spectrosc. (USSR) **48**, 46 (1980)].
[44]N. I. Koroteev, Izv. Akad. Nauk SSSR Ser. Fiz. **45**, 1504 (1981) [Bull. Acad. Sci. USSR Phys. Ser. **45**(8), 129 (1981)].
[45]L. S. Aslanyan, Resolution of Inhomogeneously Broadened Vibrational and Electronic Resonances in Liquids by the Method of Polarization Active Spectroscopy, Abstract of dissertation as candidate in the physicomathematical sciences, M. V. Lomonosov State University, M., 1981.
[46]M. D. Levenson and G. L. Eesley, IEEE J. Quantum Electron. **QE-14**, 45 (1978).
[47]C. Froehly, B. Colombean, and M. Vampouille, in: *Progress in Optics*, ed. E. Wolf, North-Holland, Amsterdam, 1983, Vol 20, p. 63.
[48]Yu. T. Mazurenko, Opt. Spektrosk. **56**, 583 (1984) [Opt. Spectrsoc. (USSR) **56**, 357 (1984)]; *ibid.* **57**, 8 (1984) [Opt. Spectrosc. (USSR) **57**, 4 (1984); Kvantovaya Elektron. (Moscow) **12**, 1235 (1985) [Sov. J. Quantum Electron. **15**, 815 (1985)]; Pis'ma Zh. Tekh. Fiz. **10**, 539 (1984) [Sov. Tech. Phys. Lett. **10**, 228 (1984)].
[49]Yu. T. Mazurenko, in: Optical Holography with Recording in Three-Dimensional Media (in Russian), ed. Yu. N. Denisyuk, Nauka, L., 1986, p. 91.
[50]A. Rebane, R. Kaarli, P. Saari, A. Anijalg, and K. Tippmann, Opt. Commun. **47**, 173 (1983); A. K. Rebane, R. K. Kaarli, and P. M. Saari, Pis'ma Zh. Eksp. Teor. Fiz. **38**, 320 (1983) [JETP Lett. **38**, 383 (1983); P. Saari and A. Rebane, Izv. Akad. Nauk ESSR Ser. Fiz. Mat. **33**, 322 (1984).
[51]A. A. Gorokhovskiĭ, R. K. Kaarli, and L. A. Rebane, Pis'ma Zh. Eksp. Teor. Fiz. **20**, 474 (1974) [JETP Lett. **20**, 216 (1974)]; B. M. Kharlamov, R. I. Personov, and L. A. Bykovskaya, Opt. Commun. **12**, 191 (1974).
[52]N. Bloembergen, see Ref. 21 (Russ. transl., 1979, p. 24).
[53]B. Ya. Zel'dovich, V. V. Shkunov, and T. V. Yakovleva, Usp. Fiz. Nauk **149**, 511 (1986) [Sov. Phys. Usp. **29**, 678 (1986)].
[54]J. K. Kauppinen, D. J. Moffatt, H. H. Mantsch, and D. G. Cameron, Appl. Spectrosc. **35**, 35, 271 (1981); Appl. Opt. **21**, 1866 (1982).
[55]H. J. Bowley, S. M. H. Collins, D. L. Gerrard, D. I. James, W. F. Maddams, P. B. Tooke, and I. D. Wyatt, Appl. Spectrosc. **39**, 1004 (1985).
[56]A. F. Bunkin, Yu. A. Khurgin, and A. Yu. Chikishev, Zh. Prikl. Spektrosk. **4**, 480 (1984) [J. Appl. Spectrosc. (USSR) **40**, 354 (1984)].
[57]L. D. Landau and E. M. Lifshits, *Electrodynamics of Continuous Media*, Pergamon Press, Oxford (1984) [Russ. original, Nauka, M., 1980].
[58]P. Price, Phys. Rev. **130**, 1792 (1983).
[59]W. J. Caspers, *ibid.* A **133**, 1249 (1964).
[60]R. W. Hellwarth, in: *Progress in Quantum Electronics*, eds., J. H. Sanders and S. Stenholm, Pergamon Press, Oxford, 1977, Vol. 5, Part 1.
[61]T. Yajima and H. Souma, Phys. Rev. **17**, 309, 324 (1978).
[62]V. M. Petnikova, S. A. Pleshanov, and V. V. Shuvalov, Zh. Eksp. Teor. Fiz. **88**, 360 (1985) [Sov. Phys. JETP **61**, 211 (1985)].
[63]S. Le Boiteux, D. Bloch, and M. Ducloy, J. Phys. (Paris) **47**, 31 (1986).
[64]D. N. Kozlov, V. V. Smirnov, and V. I. Fabelinskiĭ, Dokl. Akad. Nauk SSSR **246**, 304 (1979) [Sov. Phys. Dokl. **24**, 369 (1979)].
[65]A. Owyoung and P. Esherick, Opt. Lett. **5**, 421 (1980).
[66]V. N. Zadkov and N. I. Koroteev, Opt. Spektrosk. **59**, 67 (1985) [Opt. Spectrosc. (USSR) **59**, 40 (1985)]; V. N. Zadkov, N. I. Koroteev, M. V. Rychev, and A. B. Fedorov, Vestn. Mosk. Univ. Fiz. Astron. **24**, 45 (1984).
[67]I. L. Shumai, V. N. Zadkov, D. J. Heinzen, M. M. Kash, and M. S. Feld, Opt. Lett. **11**, 233 (1986); R. L. Farrow and R. P. Lucht, *ibid.*, p. 374.

Translated by M. V. King